



# SurvAgent: Hierarchical CoT-Enhanced Case Banking and Dichotomy-Based Multi-Agent System for Multimodal Survival Prediction

Guolin Huang<sup>1\*</sup>, Wenting Chen<sup>2\*</sup>, Jiaqi Yang<sup>3</sup>, Xinheng Lyu<sup>3</sup>,  
Xiaoling Luo<sup>1</sup>, Sen Yang<sup>4</sup>, Xiaohan Xing<sup>2†</sup>, Linlin Shen<sup>1†</sup>

<sup>1</sup>Shenzhen University, <sup>2</sup>Stanford University, <sup>3</sup>University of Nottingham Ningbo China, <sup>4</sup>Ant Group

## Abstract

Survival analysis is critical for cancer prognosis and treatment planning, yet existing methods lack the transparency essential for clinical adoption. While recent pathology agents have demonstrated explainability in diagnostic tasks, they face three limitations for survival prediction: inability to integrate multimodal data, ineffective region-of-interest exploration, and failure to leverage experiential learning from historical cases. We introduce SurvAgent, the first hierarchical chain-of-thought (CoT)-enhanced multi-agent system for multimodal survival prediction. SurvAgent consists of two stages: (1) WSI-Gene CoT-Enhanced Case Bank Construction employs hierarchical analysis through Low-Magnification Screening, Cross-Modal Similarity-Aware Patch Mining, and Confidence-Aware Patch Mining for pathology images, while Gene-Stratified analysis processes six functional gene categories. Both generate structured reports with CoT reasoning, storing complete analytical processes for experiential learning. (2) Dichotomy-Based Multi-Expert Agent Inference retrieves similar cases via RAG and integrates multimodal reports with expert predictions through progressive interval refinement. Extensive experiments on five TCGA cohorts demonstrate SurvAgent's superiority over conventional methods, proprietary MLLMs, and medical agents, establishing a new paradigm for explainable AI-driven survival prediction in precision oncology.

## 1. Introduction

Survival analysis estimates patient survival time using pathology whole slide images (WSIs) and genomic data, providing crucial insights for cancer treatment and precision medicine [14, 19]. While numerous studies [17, 35, 48–51] have achieved significant performance, existing methods

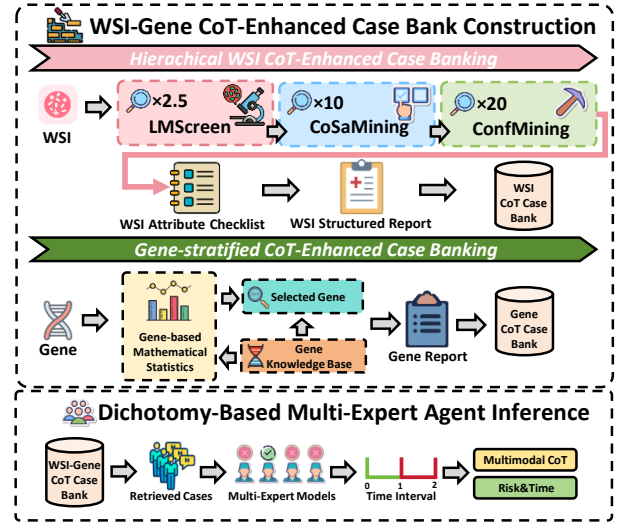


Figure 1. **SurvAgent** utilizes WSI-Gene CoT-Enhanced Case Banks through hierarchical WSI analysis and gene-stratified analysis, then performs dichotomy-based multi-expert inference by retrieving cases and progressively refining survival predictions.

lack transparent decision-making and interpretable explanations, which are essential for clinicians to validate predictions and make informed treatment decisions [1, 33]. Developing explainable multimodal survival analysis methods is therefore critical for clinical trust and adoption.

Due to the success of large language model (LLM)-based agents, they are increasingly used in medicine for various scenarios. These agents gather patient evidence, synthesize data, enable cross-specialty collaboration, and provide transparent decision-making. Pathology agents [3, 13, 28, 32, 37, 42] are developed for WSI-based diagnostics, interpretably mimicking pathologists' reasoning through operational actions (e.g., zooming, panning) while explaining their logic. However, no agent exists specifically for survival prediction, and adapting diagnostic agents to this task poses major challenges that limit performance.

\*Equal contribution.

†Corresponding Author.

First, existing pathology agents [3, 13, 28, 37, 42] primarily accept **single-modality input** (i.e., WSIs), which constrains their ability to incorporate genomic data—an essential source of molecular information for understanding tumor biology and improving survival prediction. Morphological insights from histopathology and molecular profiles from genomics offer complementary perspectives on tumor evolution and therapeutic response. Thus, integrating multimodal data within pathology agents is crucial for capturing both phenotypic and molecular determinants of prognosis, ultimately enabling more accurate and biologically informed survival prediction.

Another challenge lies in the **ineffective Region-of-Interest (ROI) exploration strategies** used by current pathology agents. Expert-based approaches [42] rely on pathologists’ viewing behaviors to identify ROIs, but this process is labor-intensive and yields limited training data, hindering scalability. Automatic methods attempt to overcome this issue but introduce new trade-offs: CPathAgent [37] downscales WSIs for efficiency at the cost of fine-grained lesion details, PathFinder [13] preserves high resolution but requires time-consuming sequential patch selection, and SlideSeek [3] employs tissue detection yet often captures irrelevant or incomplete tumor regions. Overall, existing methods either miss critical lesions, demand excessive computation, or include redundant areas, highlighting the need for an ROI mining strategy that balances accuracy, efficiency, and coverage for robust survival prediction.

Third, current pathology agents primarily analyze each test case in isolation, **overlooking valuable prognostic experience** from previous cases. Most existing agents [3, 13, 28, 37, 42] rely on pathology foundation models or case-specific knowledge bases to process WSIs independently, without leveraging information from similar patients. In contrast, clinicians often estimate survival by referencing comparable cases, highlighting the need to incorporate experiential knowledge. Although some general-purpose medical agents [18, 23–25] introduce memory or database mechanisms, they mainly store factual data while neglecting the reasoning process—how clinicians integrate and weigh evidence to reach diagnostic conclusions [7, 11, 34]. Thus, current agents need to reconstruct reasoning patterns for each new case, underscoring the importance of integrating experiential learning with explicit reasoning pathways for effective survival prediction.

To address these challenges, we introduce **SurvAgent**, the first multi-agent system specifically designed for multimodal survival prediction. Our framework consists of two key components: (1) **WSI-Gene CoT-Enhanced Case Bank Construction** for experiential learning, and (2) **Dichotomy-Based Multi-Expert Agent Inference** for final prediction.

#### WSI-Gene CoT-Enhanced Case Bank Construction

generates reasoning-based case analyses with explicit pathways for WSI and genomic data via two modules. For **effective WSI ROI exploration**, the *Hierarchical WSI CoT-Enhanced Case Bank* uses a multi-magnification pipeline: (1) At low magnification, *Low-Magnification Screening (LMScreen)*—PathAgent generates global WSI reports; (2) At medium magnification, *Cross-Modal Similarity-Aware Patch Mining (CoSMining)*—excludes redundant patches by computing self-patch and self-report similarity, selecting patches meeting both criteria; (3) At high magnification, *Confidence-Aware Patch Mining (ConfMining)*—identifies low-confidence patches, zooms in, and applies CoSMining to capture overlooked lesions. PathAgent extracts attributes via a pre-defined WSI attribute checklist, generates structured reports, and creates CoT reasoning from reports and ground-truth survival times. To **incorporate experiential learning with explicit reasoning pathways**, a self-critique and refinement mechanism stores not only patient facts but also the complete analytical reasoning process for survival prediction. The WSI CoT Case Bank stores CoTs, summarized reports, and survival times, enabling future cases to benefit from both diagnostic conclusions and reasoning processes of similar historical cases. For **multimodal data integration**, the *Gene-Stratified CoT-Enhanced Case Bank* has GenAgent analyze genomics by classifying genes into six types, performing statistical analysis, and generating type-specific reports using a knowledge base. After summarization, CoT generation, and self-critique, the Gene CoT Case Bank stores CoTs, summarized reports, and survival times alongside pathological data.

**Dichotomy-Based Multi-Expert Agent Inference** stage leverages the constructed case banks for final prediction. For test cases, the system generates hierarchical WSI reports through LMScreen, CoSMining, and ConfMining, while genomic reports are produced using the same pipeline as during case bank construction. Using retrieval-augmented generation (RAG), similar cases with their stored reasoning pathways are retrieved based on multimodal report similarity, allowing the system to reference both the conclusions and analytical processes from comparable historical cases. An inference agent then integrates retrieved cases, summarized reports, and predictions from multiple expert survival models. Rather than directly predicting survival time, the agent employs *dichotomy-based reasoning*: first classifying the case into coarse survival intervals, then progressively refining the classification, and finally predicting exact survival time within the identified interval. This hierarchical decision process, combined with comprehensive WSI-gene reports and explicit reasoning pathways, provides transparent and interpretable survival predictions that align with clinical decision-making practices. Our contributions are summarized as follows:

- We propose SurvAgent, the first multi-agent system

for multimodal survival prediction, featuring WSI-Gene CoT-Enhanced Case Banking that stores analytical reasoning processes to enable experiential learning.

- We introduce Hierarchical WSI CoT-Enhanced Case Bank with LMScreen, CoSMining, and ConfMining that balances accuracy, efficiency, and coverage across multiple magnifications.
- We propose Dichotomy-Based Multi-Expert Agent Inference that integrates retrieved cases, multimodal reports, and expert predictions through progressive interval refinement for transparent survival time prediction.
- Extensive experiments demonstrate that SurvAgent achieves the best C-index across 5 datasets while providing interpretable multimodal reports and CoT reasoning.

## 2. Related Works

### 2.1. Multimodal Survival Prediction

Current multimodal survival analysis approaches [4, 6, 17, 35, 45, 48, 48–51] integrate pathological WSIs and genomic data to provide a more comprehensive perspective on patient stratification and prognosis. For instance, Chen et al.[4] employ the Kronecker product to model pairwise feature interactions across multimodal data. Chen et al.[6] present a multimodal co-attention transformer (MCAT) framework that learns an interpretable, dense co-attention mapping between WSIs and genomic features within a unified embedding space. However, they achieve strong multimodal survival prediction performance at the expense of interpretability, lacking the transparent reasoning required for clinical trust and adoption [1, 33]. Thus, we propose a multi-agent system that enables reliable and explainable survival analysis through transparent decision-making.

### 2.2. Medical LLM-based Agent

LLM-based agents in medicine include general-purpose systems and specialty-designed agents for radiology [26, 41], gastroenterology [39], oncology [12], and pathology [3, 13, 28, 32, 37, 42]. The pathology agents perform operational actions while articulating analytical logic, but face limitations for survival prediction: they process only WSIs without integrating genomic data [3, 13, 28, 37, 42], their ROI exploration involves trade-offs between labor-intensive expert annotation [42] and automatic approaches with reduced resolution [37], excessive time [13], or irrelevant regions [3], and they analyze cases in isolation. While general-purpose agents [18, 23–25] use memory mechanisms, they store only factual data without reasoning processes. Thus, we propose a dichotomy-based multi-agent framework with cross-modal analysis, efficient patch mining for ROI selection, and WSI-Gene CoT-enhanced case banking to preserve complete prognostic reasoning.

## 3. Method

In Fig. 2, SurvAgent comprises two stages: WSI-Gene CoT-Enhanced Case Bank Construction and Dichotomy-Based Multi-Expert Agent Inference. In the first stage, we build case banks with pathological and genomic reasoning pathways. For WSI analysis, a hierarchical pipeline operates at increasing magnifications: LMScreen generates global reports at  $\times 2.5$ , CoSMining excludes redundant patches while retaining important regions at  $\times 10$  via self-patch and self-report similarity, and ConfMining identifies low-confidence patches at  $\times 20$  for further exploration. PathAgent extracts attributes using a pre-defined checklist, generates structured reports, and creates CoT reasoning with self-critique. CoTs, reports, and survival times are stored in the WSI CoT Case Bank. For genomic data, GenAgent performs gene-stratified analysis and generates type-specific reports, stored in the Gene CoT Case Bank. During inference, test cases undergo hierarchical analysis to generate multimodal reports. Using RAG, similar cases with stored CoTs are retrieved. Inference agent integrates retrieved cases, multimodal reports, and expert predictions through dichotomy-based reasoning, progressively refining survival intervals to predict exact survival time.

### 3.1. WSI-Gene CoT-Enhanced Case Bank Construction

To enable experiential learning with explicit reasoning, we construct a WSI-Gene CoT-Enhanced Case Bank that stores both patient facts and reasoning traces, mimicking how clinicians draw on experience from similar cases. It comprises two components: (1) Hierarchical WSI CoT-Enhanced Case Bank performs multi-magnification analysis through LM-Screen, CoSMining, and ConfMining to generate pathological reports and reasoning pathways, and (2) Gene-Stratified CoT-Enhanced Case Bank conducts systematic analysis across six gene types to produce genomic reports and reasoning pathways. Both components generate summarized reports, create CoT reasoning based on ground-truth survival times, apply self-critique for refinement, and store triplets into case banks for retrieval during inference.

#### 3.1.1. Hierarchical WSI CoT-Enhanced Case Bank

**Low-Magnification Screening (LMScreen).** To obtain comprehensive global understanding of the WSI while maintaining computational efficiency, we perform initial analysis at  $\times 2.5$  magnification. Given a WSI  $\mathcal{W}$ , we first downsample it to obtain the low-magnification representation  $\mathcal{W}_{2.5}$ . A PathAgent  $\mathcal{A}_{\text{wsi}}$  processes this representation to generate a global report:  $\mathcal{R}_{\text{global}} = \mathcal{A}_{\text{wsi}}(\mathcal{W}_{2.5})$ . This global report  $\mathcal{R}_{\text{global}}$  captures overall tissue architecture.

**Cross-Modal Similarity-Aware Patch Mining (CoSMining).** For effective WSI ROI exploration, we introduce CoSMining to mine fine-grained high-magnification patches by

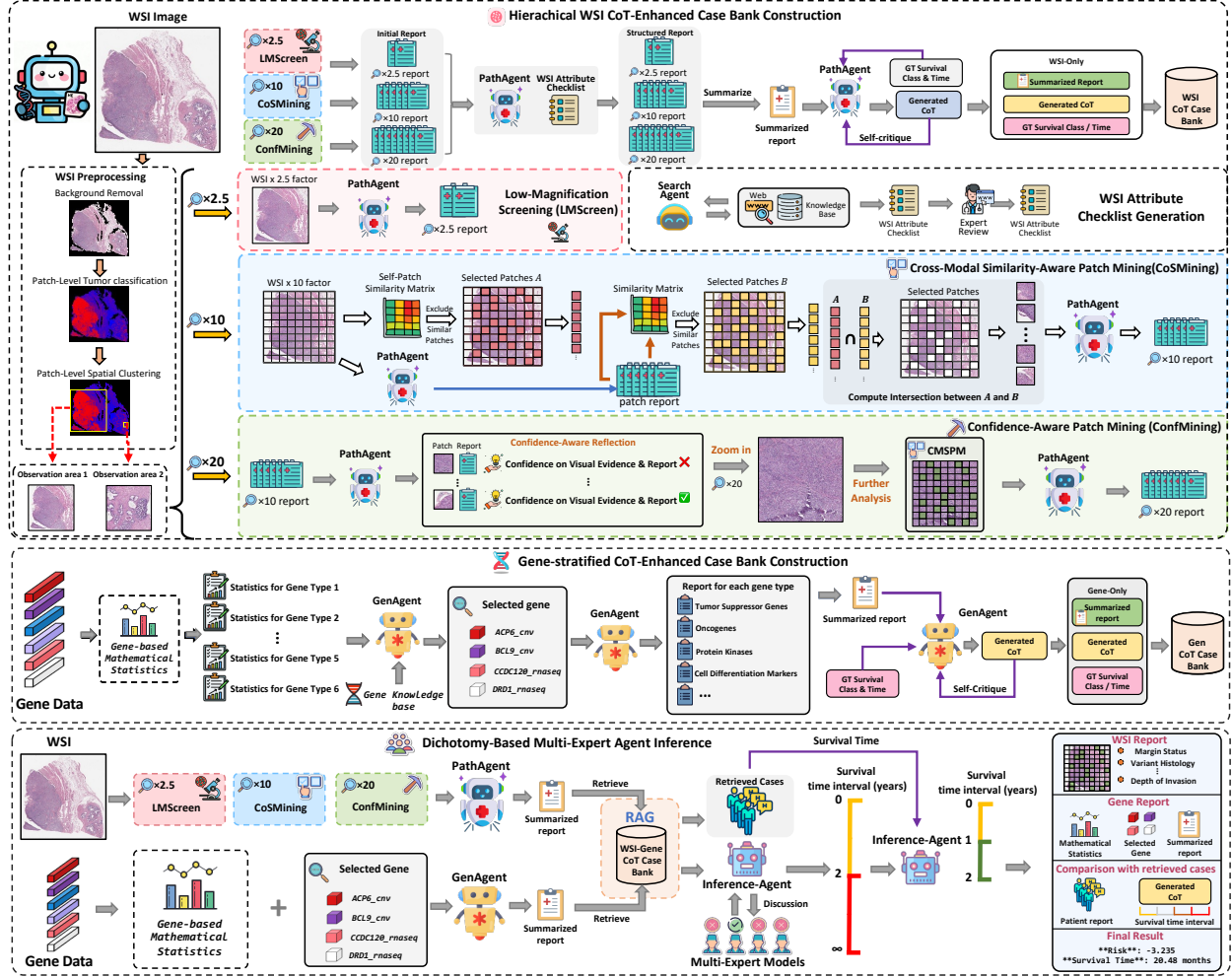


Figure 2. Overview of SurvAgent. (1) **WSI-Genes CoT-Enhanced Case Bank Construction** includes *Hierarchical WSI CoT-Enhanced Case Bank* that progressively analyzes WSIs at multiple magnifications through LMScreen, CoSMining, and ConfMining, and *Gene-Stratified CoT-Enhanced Case Bank* for gene statistical analysis. PathAgent and GenAgent generate structured reports and CoT reasoning with self-critique for their respective case banks. (2) **Dichotomy-Based Multi-Expert Agent Inference** uses RAG for retrieval and integrates retrieved cases, reports, and expert predictions for progressive survival time prediction from coarse to fine-grained intervals.

select diagnostically important patches while excluding redundant regions through self-patch and self-report similarities. Specifically, given the downsampled WSI  $\mathcal{W}_{10}$  at  $\times 10$  magnification, we partition it into  $N$  non-overlapping patches  $\{\mathbf{p}_i\}_{i=1}^N$ . To eliminate visual redundancy, we construct a self-patch similarity matrix  $\mathbf{S}^v \in \mathbb{R}^{N \times N}$ , where each element is computed as:  $S_{ij}^v = \text{sim}(\phi(\mathbf{p}_i), \phi(\mathbf{p}_j))$ , where  $\phi(\cdot)$  denotes a pathology foundation model encoder [43] and  $\text{sim}(\cdot, \cdot)$  represents cosine similarity. We identify and remove patches with high visual similarity by selecting patches whose maximum similarity to others exceeds threshold  $\tau_v$ :  $\mathcal{P}_{\text{selected}}^v = \{\mathbf{p}_i \mid \max_{j \neq i} S_{ij}^v < \tau_v\}$ .

To ensure semantic diversity, PathAgent generates preliminary reports  $\{\mathcal{R}_i\}_{i=1}^N$  for all patches. We then construct a self-report similarity matrix  $\mathbf{S}^t \in \mathbb{R}^{N \times N}$  in the textual

semantic space:  $S_{ij}^t = \text{sim}(\psi(\mathcal{R}_i), \psi(\mathcal{R}_j))$ , where  $\psi(\cdot)$  represents text embedding encoded by a text encoder [10]. Similarly, we select semantically diverse patches through the threshold  $\tau_t$ :  $\mathcal{P}_{\text{selected}}^t = \{\mathbf{p}_i \mid \max_{j \neq i} S_{ij}^t < \tau_t\}$ .

The final selected patches are obtained through intersection of both criteria:  $\mathcal{P}_{10} = \mathcal{P}_{\text{selected}}^v \cap \mathcal{P}_{\text{selected}}^t$ , ensuring patches are both visually distinctive and semantically informative. PathAgent then generates detailed reports  $\{\mathcal{R}_k\}_{k=1}^{|\mathcal{P}_{10}|}$  for these selected patches.

**Confidence-Aware Patch Mining (ConfMining).** After CoSMining identifies potentially informative patches at  $10\times$  magnification, not all patches require further high-magnification analysis. To efficiently allocate computational resources, ConfMining introduces a Confidence-Aware Reflection mechanism that selectively determines



which patches warrant deeper examination at  $20\times$  magnification based on PathAgent’s analytical confidence. For each patch  $\mathbf{p}_k \in \mathcal{P}_{10}$  with its corresponding report  $\mathcal{R}_k^{10}$ , PathAgent predicts the confidence level of the reports from three categories: low, medium, and high. When PathAgent assigns a low confidence level—indicating uncertainty about morphological features, ambiguous cellular patterns, or the need for finer details—the patch is selected for hierarchical  $20\times$  magnification analysis.

For each low-confidence patch  $\mathbf{p}_k \in \mathcal{P}_{\text{low-conf}}$ , we zoom in to  $\times 20$  magnification to obtain its high-resolution version  $\mathbf{p}_k^{20}$  and partition it into  $M$  sub-patches  $\{\mathbf{p}_{k,m}^{20}\}_{m=1}^M$ . To avoid exhaustive analysis of all sub-patches, we apply the CoSMining strategy at this finer scale to extract the most informative sub-patches through cross-modal similarity filtering:  $\mathcal{P}_k^{20} = \text{CoSMining}(\mathbf{p}_k^{20}; \tau_v, \tau_t)$ . The final set of high-magnification patches is  $\mathcal{P}_{20} = \bigcup_k \mathcal{P}_k^{20}$ , and PathAgent generates corresponding detailed reports  $\{\mathcal{R}_m^{20}\}_{m=1}^{|\mathcal{P}_{20}|}$  for these selected sub-patches. This two-stage confidence-driven and similarity-aware mining process ensures thorough analysis of uncertain regions while maintaining computational efficiency by focusing only on the most relevant fine-grained features within low-confidence patches.

**WSI Attribute Checklist Generation.** To ensure structured and clinically relevant analysis, we employ a search agent  $\mathcal{A}_{\text{search}}$  to establish a WSI attribute checklist  $\mathcal{C}_{\text{WSI}}$ . The search agent queries medical knowledge bases  $\mathcal{K}_{\text{med}}$  [28] and online resources  $\mathcal{D}_{\text{web}}$  [30] to identify prognostically important attributes:  $\mathcal{C}_{\text{raw}} = \mathcal{A}_{\text{search}}(\mathcal{K}_{\text{med}}, \mathcal{D}_{\text{web}}; q_{\text{survival}})$ , where  $q_{\text{survival}}$  represents survival-prediction-specific queries. The raw checklist  $\mathcal{C}_{\text{raw}}$  is then reviewed and refined by clinical experts to obtain  $\mathcal{C}_{\text{WSI}} = \{a_1, a_2, \dots, a_K\}$ , where each  $a_k$  represents a key pathological attribute (e.g., tumor grade, necrosis extent, lymphocytic infiltration). We include 16 key attributes.

Using this checklist, PathAgent extracts structured information from all hierarchical reports:

$$\mathcal{R}_{\text{struct}} = \mathcal{A}_{\text{wsi}}(\{\mathcal{R}_{\text{global}}\}, \{\mathcal{R}_k^{10}\}, \{\mathcal{R}_m^{20}\}; \mathcal{C}_{\text{WSI}}),$$

and generates a summarized report  $\mathcal{R}_{\text{sum}}^{\text{WSI}}$  by removing redundant information. Finally, given the summarized report  $\mathcal{R}_{\text{sum}}^{\text{WSI}}$  and GT survival time  $t_{\text{GT}}$ , PathAgent generates CoT reasoning:  $\text{CoT}_{\text{WSI}} = \mathcal{A}_{\text{wsi}}(\mathcal{R}_{\text{sum}}^{\text{WSI}}, t_{\text{GT}})$ .

To ensure the correctness of the CoT, we utilize a self-critique mechanism to evaluate the generated CoT. Specifically, we employ Qwen2.5-32B as the quality validation function  $\mathcal{V}(\cdot)$  to assess the CoT and generate both a quality level (low or high) and detailed critique. The refinement process is formulated as:

$$\text{CoT}_{\text{WSI}}^{\text{refined}} = \begin{cases} \text{CoT}_{\text{WSI}} & \text{if } \mathcal{V}(\text{CoT}_{\text{WSI}}) = \text{high} \\ \mathcal{A}_{\text{wsi}}(\text{CoT}_{\text{WSI}}, \text{Critique}) & \text{Otherwise} \end{cases}, \quad (1)$$

where  $\mathcal{V}(\text{CoT}_{\text{WSI}})$  returns the quality level and generates a critique, and  $\mathcal{A}_{\text{wsi}}(\cdot, \cdot)$  denotes PathAgent’s refinement operation that revises the CoT based on critique feedback until high quality is achieved. The final triplet  $(\mathcal{R}_{\text{sum}}^{\text{WSI}}, \text{CoT}_{\text{WSI}}^{\text{refined}}, t_{\text{GT}})$  is stored in the WSI CoT Case Bank  $\mathcal{B}_{\text{WSI}}$ . Through this hierarchical pipeline, from global screening to cross-modal mining and confidence-aware refinement, we construct a comprehensive WSI case bank capturing multi-scale morphological features with explicit reasoning pathways for experiential survival prediction.

### 3.1.2. Gene-Stratified CoT-Enhanced Case Bank

For multimodal data integration, we introduce a Gene-Stratified CoT-Enhanced Case Bank to systematically analyze genomic data. Since raw genomic data is highly abstract with individual genes often lacking direct clinical value, we classify genes by functional roles into six prognostically important categories: Tumor Suppressor Genes, Oncogenes, Protein Kinases, Cell Differentiation Markers, Transcription Factors, and Cytokines and Growth Factors. Given genomic data  $\mathcal{G}$ , let  $\mathcal{G}_l$  denote the gene subset of type  $l$  where  $l = \{1, \dots, L\}$ , ( $L = 6$ ). For each type, we compute statistical features  $\mathbf{s}_l = [\mu_l, m_l, r_{\text{mut}}^l]$ , where  $\mu_l$ ,  $m_l$ , and  $r_{\text{mut}}^l$  represent mean expression, median, and mutation ratio, providing comprehensive quantitative characterization of expression and mutation patterns.

These statistics are submitted to GenAgent  $\mathcal{A}_{\text{gen}}$  for preliminary analysis. GenAgent analyzes the statistical information with gene knowledge base  $\mathcal{K}_{\text{gene}}$  [44] to autonomously select genes with significant prognostic impact,  $\mathcal{G}_l^* = \mathcal{A}_{\text{gen}}^{\text{select}}(\mathbf{s}_l, \mathcal{G}_l; \mathcal{K}_{\text{gene}})$ , where  $\mathcal{G}_l^* \subset \mathcal{G}_l$  contains selected important genes. GenAgent then retrieves raw expression data and consults  $\mathcal{K}_{\text{gene}}$  to understand each gene’s implications. Through coarse-to-fine analysis from statistics to gene details, GenAgent produces type-specific reports,  $\mathcal{R}_l^{\text{gene}} = \mathcal{A}_{\text{gen}}^{\text{report}}(\mathbf{s}_l, \mathcal{G}_l^*; \mathcal{K}_{\text{gene}})$ .

After analyzing all six categories, GenAgent generates a comprehensive genomic report  $\mathcal{R}_{\text{sum}}^{\text{gene}}$ . Similar to WSI analysis, GenAgent generates CoT reasoning from the genomic report and GT patient survival class and time:  $\text{CoT}_{\text{gene}} = \mathcal{A}_{\text{gen}}(\mathcal{R}_{\text{sum}}^{\text{gene}}, t_{\text{GT}})$ , followed by self-critique and refinement:

$$\text{CoT}_{\text{gene}}^{\text{refined}} = \begin{cases} \text{CoT}_{\text{gene}} & \text{if } \mathcal{V}(\text{CoT}_{\text{gene}}) = \text{high} \\ \mathcal{A}_{\text{gen}}(\text{CoT}_{\text{gene}}, \text{Critique}) & \text{Otherwise} \end{cases}. \quad (2)$$

The triplet  $(\mathcal{R}_{\text{sum}}^{\text{gene}}, \text{CoT}_{\text{gene}}^{\text{refined}}, t_{\text{GT}})$  is stored in Gene CoT Case Bank  $\mathcal{B}_{\text{gene}}$  for inference-time retrieval. Through this gene-stratified pipeline, from statistical characterization to targeted gene selection and CoT-enhanced analysis, we construct a comprehensive genomic case bank capturing functional genomic patterns with explicit reasoning pathways for knowledge-guided survival prediction.

Table 1. Comparison of survival prediction performance (C-index) across different models and modalities on five TCGA cancer cohorts. G: Genomic modality, H: Histopathology modality. “\*” indicate best results from our reimplementation; Others are from original publications.

Model	Modality	BLCA (N = 373)	BRCA (N = 956)	GBMLGG (N = 480)	LUAD (N = 569)	UCEC (N = 453)	Overall
Conventional Methods							
SNN* [21]	G	0.541±0.016	0.466±0.058	0.598±0.054	0.539±0.069	0.493±0.096	0.527
SNNTrans [50]	G	0.646±0.043	0.648±0.058	0.828±0.016	0.634±0.049	0.632±0.032	0.678
AttnMIL [16, 50]	H	0.605±0.045	0.551±0.077	0.816±0.011	0.563±0.050	0.614±0.052	0.630
MaxMIL [50]	H	0.551±0.032	0.597±0.055	0.714±0.057	0.596±0.060	0.563±0.055	0.604
DeepAttnMISL [45, 46]	H	0.504±0.042	0.524±0.043	0.734±0.029	0.548±0.050	0.597±0.059	0.581
M3IF [22, 50]	G+H	0.636±0.020	0.620±0.071	0.824±0.017	0.630±0.031	0.667±0.029	0.675
HFBSurv [50]	G+H	0.640±0.028	0.647±0.035	0.838±0.013	0.650±0.050	0.642±0.045	0.683
MOTCat* [45]	G+H	0.674±0.024	0.684±0.011	0.831±0.028	0.674±0.036	0.667±0.051	0.706
MCAT* [5]	G+H	0.645±0.053	0.601±0.069	<b>0.852±0.028</b>	0.636±0.043	0.634±0.018	0.674
CCL* [50]	G+H	0.652±0.034	0.593±0.058	0.845±0.012	0.640±0.059	0.668±0.041	0.680
Proprietary MLLMs							
Gemini-2.5-Pro* [8]	G+H	0.572±0.031	0.555±0.055	0.551±0.026	0.531±0.062	0.498±0.067	0.541
Claude-4.5* [2]	G+H	0.545±0.027	0.555±0.046	0.505±0.053	0.509±0.059	0.479±0.034	0.519
GPT-5* [31]	G+H	0.576±0.038	0.434±0.057	0.493±0.053	0.510±0.087	0.495±0.083	0.502
Medical Agents							
MDAgent* [20]	G+H	0.558±0.040	0.482±0.064	0.495±0.040	0.524±0.064	0.509±0.049	0.514
MedAgent* [38]	G+H	0.515±0.039	0.510±0.031	0.483±0.020	0.485±0.050	0.551±0.066	0.509
<b>SurvAgent (Ours)</b>	G+H	<b>0.683±0.022</b>	<b>0.695±0.013</b>	0.833±0.029	<b>0.676 ± 0.036</b>	<b>0.676±0.052</b>	<b>0.713</b>

### 3.2. Dichotomy-Based Multi-Expert Agent Inference Stage

For a test case with WSI  $\mathcal{W}_{\text{test}}$  and genomic data  $\mathcal{G}_{\text{test}}$ , we first generate multimodal reports using the same hierarchical pipeline. For WSI analysis, we apply the hierarchical analysis pipeline including LMScreen, CoSMining, and ConfMining to extract hierarchal WSI reports  $\mathcal{R}_{\text{test}}^{\text{WSI}}$ . For genomic data, we perform gene-stratified analysis across six gene types to characterize genomic reports  $\mathcal{R}_{\text{test}}^{\text{gene}}$ .

Using retrieval-augmented generation (RAG), we retrieve  $K$  similar cases from both case banks based on multimodal report similarity:

$$\mathcal{B}_{\text{retrieved}} = \text{RAG}(\mathcal{R}_{\text{test}}^{\text{WSI}}, \mathcal{R}_{\text{test}}^{\text{gene}}; \mathcal{B}_{\text{WSI}}, \mathcal{B}_{\text{gene}}, K), \quad (3)$$

where each retrieved case contains its summarized reports, CoT reasoning, and survival class and time.

Additionally, we collect predictions from  $M$  expert survival models [6, 45, 50]:  $\{\hat{t}_m\}_{m=1}^M = \{\mathcal{M}_m(\mathcal{W}_{\text{test}}, \mathcal{G}_{\text{test}})\}_{m=1}^M$ , where  $\mathcal{M}_m$  represents the  $m$ -th expert model. The inference agent  $\mathcal{A}_{\text{infer}}$  performs dichotomy-based reasoning by progressively refining survival intervals. We define a hierarchical interval structure with  $D$  dichotomy levels. At the first level, the agent performs coarse classification:

$$y_1 = \mathcal{A}_{\text{infer}}(\mathcal{B}_{\text{retrieved}}, \mathcal{R}_{\text{test}}^{\text{WSI}}, \mathcal{R}_{\text{test}}^{\text{gene}}, \{\hat{t}_m\}; \text{level} = 1), \quad (4)$$

where  $y_1 \in \{1, 2\}$  divides cases into two broad survival categories. At each subsequent level  $d = \{2, \dots, D\}$ , the agent further refines the classification within the selected

interval:

$$y_d = \mathcal{A}_{\text{infer}}(\mathcal{B}_{\text{retrieved}}, \mathcal{R}_{\text{test}}^{\text{WSI}}, \mathcal{R}_{\text{test}}^{\text{gene}}, \{\hat{t}_m\}, y_{d-1}; \text{level} = d), \quad (5)$$

progressively narrowing the survival interval until reaching the finest granularity. Finally, the exact survival time is predicted within the identified interval:

$$\hat{t}_{\text{final}} = \mathcal{A}_{\text{infer}}(\mathcal{B}_{\text{retrieved}}, \mathcal{R}_{\text{test}}^{\text{WSI}}, \mathcal{R}_{\text{test}}^{\text{gene}}, \{\hat{t}_m\}, y_D). \quad (6)$$

The inference agent outputs comprehensive results including the predicted survival time  $\hat{t}_{\text{final}}$ , multimodal reports ( $\mathcal{R}_{\text{test}}^{\text{WSI}}, \mathcal{R}_{\text{test}}^{\text{gene}}$ ), and an inference reasoning report  $\mathcal{R}_{\text{reasoning}}$  that documents the complete decision-making process, providing transparency for clinical validation.

## 4. Experiments

### 4.1. Datasets and Settings

**Datasets and Evaluation.** To ensure fair comparison, we follow prior protocols using five-fold cross-validation on five datasets: Bladder Urothelial Carcinoma (BLCA), Breast Invasive Carcinoma (BRCA), Glioblastoma and Lower Grade Glioma (GBMLGG), Lung Adenocarcinoma (LUAD), and Uterine Corpus Endometrial Carcinoma (UCEC). Data volumes remain consistent across datasets (details in Table 1). We evaluate using the Concordance Index (C-index)[15], Kaplan-Meier survival curves[19], and Log-rank test [29] to assess survival differences between risk groups and validate prediction reliability.

**Implementation.** For each WSI, tissue regions are segmented via Otsu’s thresholding. Non-overlapping  $256 \times 256$

Table 2. Ablation study of different components in SurvAgent framework.

WSI CoT bank	Gene CoT bank	Inference	BLCA	BRCA	GBMLGG	LUAD	UCEC	Overall
			0.452±0.030	0.421±0.033	0.463±0.024	0.498±0.086	0.470±0.045	0.461
✓			0.612±0.053	0.542±0.095	0.791±0.024	0.559±0.039	0.585±0.050	0.618
	✓		0.539±0.016	0.455±0.056	0.591±0.050	0.545±0.073	0.481±0.082	0.522
		✓	0.664±0.041	0.665±0.012	0.813±0.024	0.650±0.039	0.652±0.052	0.689
✓	✓	✓	<b>0.683±0.022</b>	<b>0.695±0.013</b>	<b>0.833±0.029</b>	<b>0.676±0.033</b>	<b>0.676±0.052</b>	<b>0.713</b>

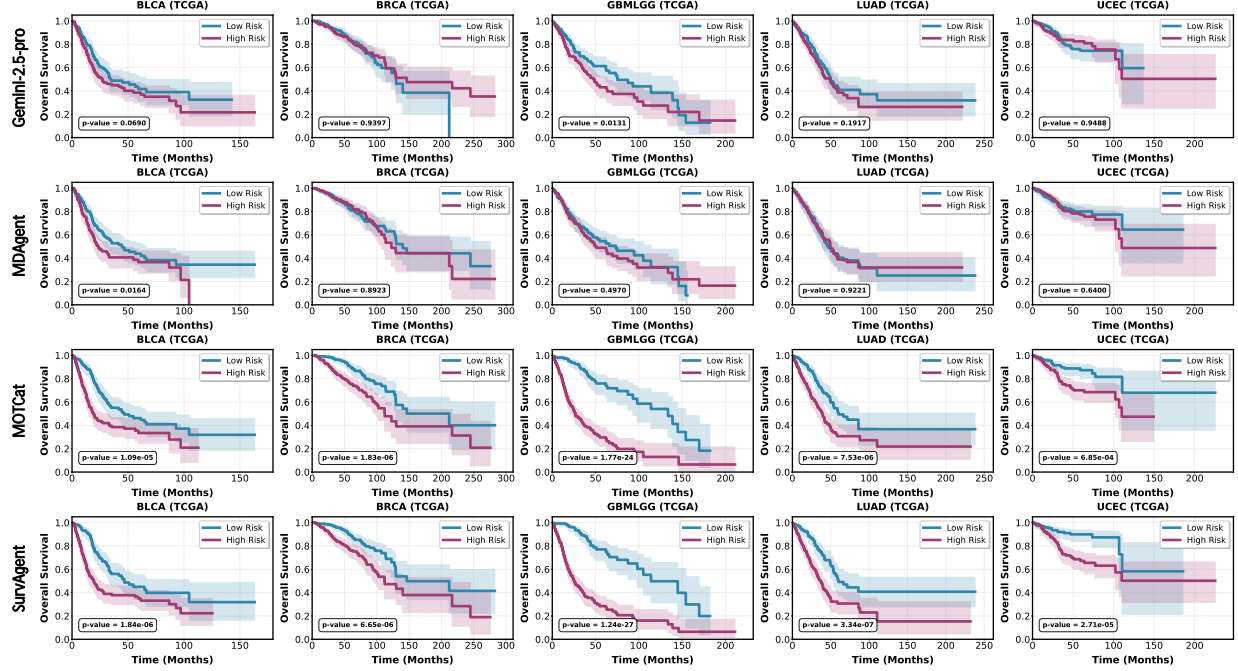


Figure 3. Kaplan-Meier Analysis of predicted high-risk (red) and low-risk (blue) groups on five cancer datasets and their p-values. Shaded areas refer to the confidence intervals.

patches are extracted from tissue areas at  $20\times$  magnification and processed with CLAM [27] to extract features for survival prediction models. Genomic data uses an SNN [21] encoder. CoSMining parameters:  $\tau_v = \tau_t = 0.93$ ; RAG:  $K = 3$ ; inference:  $D = 2$ . Code will be publicly released.

## 4.2. Comparison with State-of-the-Arts

To prove the superiority of our SurvAgent, we compare it against SOTA approaches across five TCGA cancer cohorts in survival prediction, including conventional methods (unimodal and multimodal), leading proprietary MLLMs (Gemini 2.5 Pro [8], Claude 4.5 [2], GPT-5 [31]), and medical multi-agent systems (MedAgent [38] and MDAgent [20]), as shown in Table 1.

**Comparison with Conventional Methods.** Our SurvAgent demonstrates superior performance over conventional survival prediction methods across most cohorts. Compared to the best conventional baseline MOTCat, SurvAgent achieves improvements of 0.9%, 1.1%, and 0.2% in C-index on BLCA, BRCA, and LUAD, respec-

tively, with 0.7% overall gain. Compared to unimodal approaches, SurvAgent significantly surpasses genomic-based (SNNTrans: 0.678) and histopathology-based methods (AttnMIL: 0.630). The key advantage lies in our hierarchical WSI analysis and CoT-enhanced case banking enabling experiential learning, unlike conventional feature fusion methods, leading to more robust predictions.

**Comparison with Proprietary MLLMs.** General-purpose proprietary MLLMs exhibit poor performance on survival prediction despite advanced capabilities elsewhere. Our SurvAgent substantially outperforms Gemini-2.5-Pro, Claude-4.5, and GPT-5 by 17.2%, 19.4%, and 21.1% in overall C-index. On GBMLGG, the gap is most pronounced: SurvAgent achieves 0.833 versus Gemini-2.5-Pro (0.551), Claude-4.5 (0.505), and GPT-5 (0.493). Even where proprietary MLLMs perform relatively better, such as Gemini-2.5-Pro on BLCA (0.572), SurvAgent achieves 11.1% gains. These results show that general MLLMs struggle with medical prediction tasks requiring domain

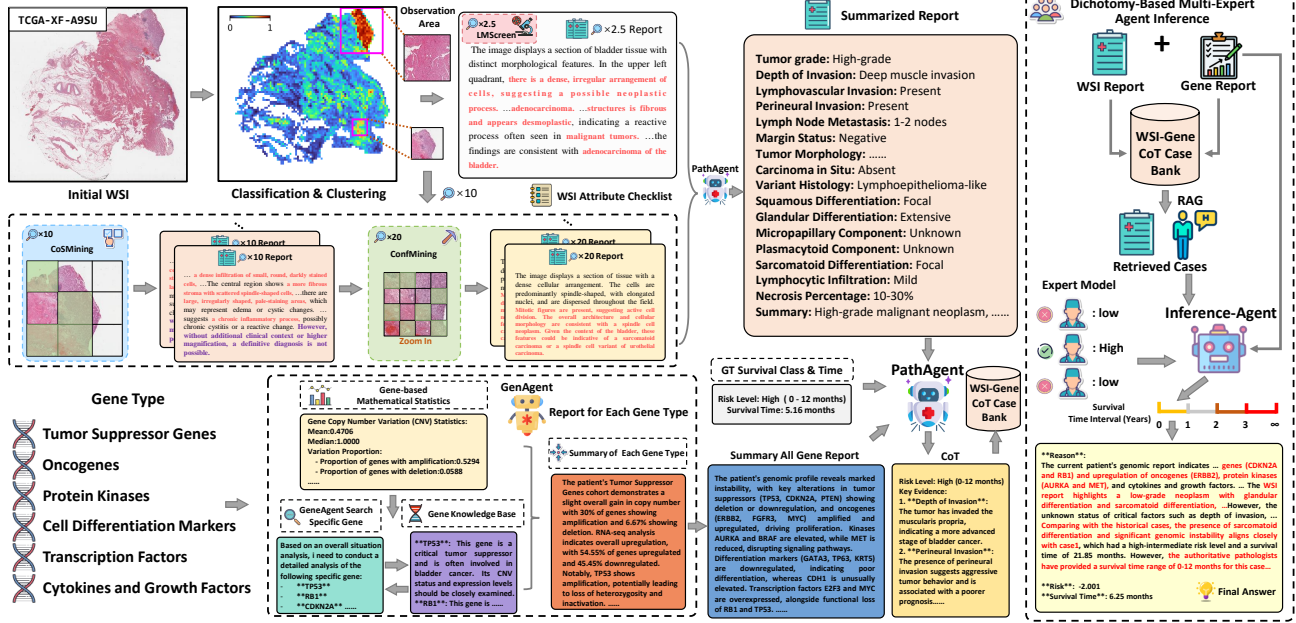


Figure 4. Explainability analysis through visualization on case TCGA-XF-A9SU

knowledge and structured multimodal reasoning, highlighting the need for specialized models like SurvAgent.

**Comparison with Medical Multi-Agent Systems.** Our SurvAgent significantly outperforms existing medical multi-agent systems, achieving 19.9% and 20.4% overall C-index improvements over MDAgent and MedAgent. Across all cohorts, SurvAgent consistently demonstrates superior performance: improvements range from 12.5% (BLCA) to 33.8% (GBMLGG) over MDAgent, and 16.8% (BLCA) to 35.0% (GBMLGG) over MedAgent. These substantial gaps highlight advantages of our task-specific design: modality-specific agents, CoT-enhanced case banking for experiential learning, and dichotomy-based inference for transparent decisions, demonstrating that domain-specific multi-agent architectures significantly outperform general-purpose medical agents in complex clinical prediction.

### 4.3. Ablation Study

To evaluate the effectiveness of each proposed component, we conduct ablation studies by systematically removing individual modules. In Table 2, SurvAgent comprises three main components: the Hierarchical WSI CoT-Enhanced Case Bank, the Gene-Stratified CoT-Enhanced Case Bank, and the Dichotomy-Based Multi-Expert Agent Inference stage. When integrating only the WSI CoT bank with baseline survival models, the overall C-index improves from 0.461 to 0.618, showing the substantial value of hierarchical pathological case-based reasoning. Similarly, incorporating only the Gene CoT bank yields an overall C-index of

0.522, confirming that genomic experiential learning also contributes to performance improvement. When incorporating the proposed inference pipeline, the performance of baseline model boosts by 0.22 in C-index, suggesting its effectiveness. The complete SurvAgent framework, which integrates both case banks with dichotomy-based multi-agent inference, achieves the highest overall C-index of 0.713, demonstrating the synergistic benefits of multimodal case-based reasoning and progressive interval refinement.

### 4.4. Patient Stratification

Beyond C-index, patient stratification into distinct risk subgroups is critical for cancer prognosis. We compared SurvAgent with top models from each category: MOTCat (conventional), Gemini-2.5-pro (MLLM), and MDAgent (multi-agent) using Kaplan-Meier curves (Fig. 3). MLLMs and multi-agent frameworks failed to discriminate high-risk from low-risk populations effectively. Gemini-2.5-pro and MDAgent showed non-significant results ( $p > 0.05$ ) on 80% (4/5) of datasets, indicating unstable feature-outcome associations. SurvAgent achieved 100% statistical significance (all  $p < 0.05$ ). On GBMLGG, SurvAgent demonstrated exceptional stratification ( $p = 1.24e-27$ ). Compared to MOTCat, SurvAgent achieved comparable or better p-values, demonstrating its ability to leverage WSI and genomic features for robust survival prediction. This performance derives from our WSI-Gene CoT-Enhanced Case Bank and Dichotomy-Based Multi-Agent Inference, which together enable interpretable, accurate, and progressively



refined risk stratification.

#### 4.5. Explainability Analysis

To demonstrate the explainability and accuracy of SurvAgent, we present a comprehensive case study in the Fig.1 for case TCGA-XF-A9SU. The hierarchical WSI analysis begins with LMScreen identifying adenocarcinoma with “dense, irregular arrangement of cells” and desmoplastic structures. CoSMining’s  $\times 10$  report reveals “dense infiltration of small, round, darkly stained cells” with fibrous stroma and spindle-shaped cells, noting “without additional clinical context or higher magnification, a definitive diagnosis is not possible.” ConfMining’s  $\times 20$  report then identifies critical features: “predominantly spindle-shaped cells with elongated nuclei” and “mitotic figures present,” with morphology “consistent with spindle cell neoplasm indicative of sarcomatoid carcinoma”—prompting higher magnification analysis. The WSI Attribute Checklist extracts 15 features including deep muscle invasion, perineural invasion, and focal sarcomatoid differentiation, summarizing as “high-grade malignant neoplasm with perineural invasion and necrosis.” GenAgent analyzes genes (TP53, RB1, CDKN2A), revealing “TP53 amplification potentially leading to loss of heterozygosity,” “marked instability with tumor suppressors (TP53, CDKN2A, PTEN) deletion/downregulation, oncogenes (ERBB2, FGFR3, MYC) amplified/upregulated,” and “overexpressed E2F3/MYC with functional loss of RB1/TP53.” The CoT reasoning documents muscularis propria invasion and perineural invasion as aggressive indicators, classifying as high-risk (0-12 months) the same as the GT low-risk labeling (5.16 months). The final inference agent reconciles conflicting signals—e.g., “sarcomatoid differentiation and genomic instability align with case1 (21.85 months), but experts estimate 0–12 months”—and through dichotomy-based reasoning predicts 6.25 months (risk =  $-2.001$ ) versus the ground truth 5.16 months, transparently balancing contradictory evidence for interpretable clinical reasoning.

#### 5. Conclusion


We present SurvAgent, the first multi-agent system for multimodal survival prediction. Through WSI-Gene CoT-Enhanced Case Banking, we enable experiential learning by storing analytical reasoning processes from historical cases. Our hierarchical pipeline balances accuracy, efficiency, and coverage via LMScreen, CoSMining, and ConfMining, while dichotomy-based inference ensures transparent predictions. Extensive experiments show our superiority to conventional methods, MLLMs, and medical agents with consistent statistical significance in patient stratification.

#### References

- [1] Qaiser Abbas, Woonyoung Jeong, and Seung Won Lee. Explainable ai in clinical decision support systems: A meta-analysis of methods, applications, and usability challenges. In *Healthcare*, page 2154. MDPI, 2025. 1, 3
- [2] Anthropic. Claude 4.5 [large language model], 2025. Accessed 2025-11-14. 6, 7
- [3] Chengkuan Chen, Luca L Weishaupt, Drew FK Williamson, Richard J Chen, et al. Evidence-based diagnostic reasoning with multi-agent copilot for human pathology. *arXiv preprint arXiv:2506.20964*, 2025. 1, 2, 3
- [4] Richard J Chen, Ming Y Lu, Jingwen Wang, Drew FK Williamson, Scott J Rodig, Neal I Lindeman, and Faisal Mahmood. Pathomic fusion: an integrated framework for fusing histopathology and genomic features for cancer diagnosis and prognosis. *IEEE Transactions on Medical Imaging*, 41(4):757–770, 2020. 3
- [5] Richard J. Chen, Ming Y. Lu, Wei-Hung Weng, Tiffany Y. Chen, Drew F.K. Williamson, Trevor Manz, Maha Shady, and Faisal Mahmood. Multimodal co-attention transformer for survival prediction in gigapixel whole slide images. In *Proceedings of the IEEE/CVF International Conference on Computer Vision (ICCV)*, pages 4015–4025, 2021. 6
- [6] Richard J Chen, Ming Y Lu, Wei-Hung Weng, Tiffany Y Chen, Drew FK Williamson, Trevor Manz, Maha Shady, and Faisal Mahmood. Multimodal co-attention transformer for survival prediction in gigapixel whole slide images. In *Proceedings of the IEEE/CVF international conference on computer vision*, pages 4015–4025, 2021. 3, 6
- [7] Justin J Choi, Jeanie Gribben, Myriam Lin, Erika L Abramson, and Juliet Aizer. Using an experiential learning model to teach clinical reasoning theory and cognitive bias: an evaluation of a first-year medical student curriculum. *Medical Education Online*, 28(1):2153782, 2023. 2
- [8] Google DeepMind. Gemini 2.5 pro [large language model], 2025. Accessed 2025-11-14. 6, 7
- [9] DeepSeek-AI et al. Deepseek-v3 technical report, 2025. 3
- [10] Jacob Devlin, Ming-Wei Chang, Kenton Lee, and Kristina Toutanova. Bert: Pre-training of deep bidirectional transformers for language understanding. In *Proceedings of the 2019 conference of the North American chapter of the association for computational linguistics: human language technologies, volume 1 (long and short papers)*, pages 4171–4186, 2019. 4
- [11] Joseph H Donroe, Emilie Egger, Sarita Soares, Andre N So-fair, and John Moriarty. Clinical reasoning: Perspectives of expert clinicians on reasoning through complex clinical cases. *Cureus*, 16(1), 2024. 2
- [12] Dyke Ferber, Omar SM El Nahhas, Georg Wölflein, Isabella C Wiest, et al. Development and validation of an autonomous artificial intelligence agent for clinical decision-making in oncology. *Nature cancer*, pages 1–13, 2025. 3
- [13] Fatemeh Ghezloo, Mehmet Saygin Seyfioglu, Rustin Soraki, Wisdom O Ikezogwo, Beibin Li, Tejoram Vivekanandan, Joann G Elmore, Ranjay Krishna, and Linda Shapiro. Pathfinder: A multi-modal multi-agent system for medical

- diagnostic decision-making applied to histopathology. *arXiv preprint arXiv:2502.08916*, 2025. 1, 2, 3
- [14] Balázs Györfy. Survival analysis across the entire transcriptome identifies biomarkers with the highest prognostic power in breast cancer. *Computational and structural biotechnology journal*, 19:4101–4109, 2021. 1
- [15] Frank E Harrell Jr, Kerry L Lee, and Daniel B Mark. Multivariable prognostic models: issues in developing models, evaluating assumptions and adequacy, and measuring and reducing errors. *Statistics in medicine*, 15(4):361–387, 1996. 6
- [16] Maximilian Ilse, Jakub M. Tomczak, and Max Welling. Attention-based deep multiple instance learning, 2018. 6
- [17] Guillaume Jaume, Anurag Vaidya, Richard J Chen, Drew FK Williamson, Paul Pu Liang, and Faisal Mahmood. Modeling dense multimodal interactions between biological pathways and histology for survival prediction. In *Proceedings of the IEEE Conf. Comput. Vis. Pattern Recognit.*, pages 11579–11590, 2024. 1, 3
- [18] Xun Jiang, Feng Li, Han Zhao, Jiahao Qiu, Jiaying Wang, et al. Long term memory: The foundation of ai self-evolution. *arXiv preprint arXiv:2410.15665*, 2024. 2, 3
- [19] Edward L Kaplan and Paul Meier. Nonparametric estimation from incomplete observations. *Journal of the American statistical association*, 53(282):457–481, 1958. 1, 6
- [20] Yubin Kim, Chanwoo Park, Hyewon Jeong, Yik S Chan, Xuhai Xu, Daniel McDuff, Hyeonhoon Lee, Marzyeh Ghassemi, Cynthia Breazeal, and Hae W Park. Mdagents: An adaptive collaboration of llms for medical decision-making. *Advances in Neural Information Processing Systems*, 37:79410–79452, 2024. 6, 7
- [21] Günter Klambauer, Thomas Unterthiner, Andreas Mayr, and Sepp Hochreiter. Self-normalizing neural networks. *Advances in neural information processing systems*, 30, 2017. 6, 7
- [22] Hang Li, Fan Yang, Xiaohan Xing, Yu Zhao, Jun Zhang, Yueping Liu, Mengxue Han, Junzhou Huang, Liansheng Wang, and Jianhua Yao. Multi-modal multi-instance learning using weakly correlated histopathological images and tabular clinical information. In *Medical Image Computing and Computer Assisted Intervention – MICCAI 2021*, pages 529–539, Cham, 2021. Springer International Publishing. 6
- [23] Junkai Li, Yunghwei Lai, Weitao Li, Jingyi Ren, et al. Agent hospital: A simulacrum of hospital with evolvable medical agents. *arXiv preprint arXiv:2405.02957*, 2024. 2, 3
- [24] Rumeng Li, Xun Wang, Dan Berlowitz, Jesse Mez, Honghuang Lin, and Hong Yu. Care-ad: a multi-agent large language model framework for alzheimer’s disease prediction using longitudinal clinical notes. *npj Digital Medicine*, 8(1):541, 2025.
- [25] Jie Liu, Wenxuan Wang, Zizhan Ma, Guolin Huang, Yihang SU, Kao-Jung Chang, Wenting Chen, Haoliang Li, Linlin Shen, and Michael Lyu. Medchain: Bridging the gap between llm agents and clinical practice through interactive sequential benchmarking. *arXiv preprint arXiv:2412.01605*, 2024. 2, 3
- [26] Jinhui Lou, Yan Yang, Zhou Yu, Zhenqi Fu, Weidong Han, Qingming Huang, and Jun Yu. Cxragent: Director-orchestrated multi-stage reasoning for chest x-ray interpretation. *arXiv preprint arXiv:2510.21324*, 2025. 3
- [27] Ming Y Lu, Drew FK Williamson, Tiffany Y Chen, Richard J Chen, Matteo Barbieri, and Faisal Mahmood. Data-efficient and weakly supervised computational pathology on whole-slide images. *Nature biomedical engineering*, 5(6):555–570, 2021. 7, 3
- [28] Xinheng Lyu, Yuci Liang, Wenting Chen, Meidan Ding, Jiaqi Yang, Guolin Huang, Daokun Zhang, Xiangjian He, and Linlin Shen. Wsi-agents: A collaborative multi-agent system for multi-modal whole slide image analysis. In *International Conference on Medical Image Computing and Computer-Assisted Intervention*, pages 680–690, 2025. 1, 2, 3, 5
- [29] Nathan Mantel et al. Evaluation of survival data and two new rank order statistics arising in its consideration. *Cancer Chemother Rep*, 50(3):163–170, 1966. 6
- [30] MyPathologyReport Team. My pathology report — patient pathology (traditional chinese). <https://www.mypathologyreport.ca/zh-TW/>, 2025. Internationally recognized, pathologist-written and peer-reviewed patient education resource; disclaimer: content is for general information, not individualized medical advice. 5
- [31] OpenAI. Gpt-5 (version 2025-08-07) [large language model], 2025. Accessed 2025-11-14. 6, 7
- [32] Ngoc Bui Lam Quang, Nam Le Nguyen Binh, Thanh-Huy Nguyen, Le Thien Phuc Nguyen, Quan Nguyen, and Ulas Bagci. Gmat: Grounded multi-agent clinical description generation for text encoder in vision-language mil for whole slide image classification. In *International Workshop on Emerging LLM/LMM Applications in Medical Imaging*, pages 1–9. Springer, 2025. 1, 3
- [33] Tim Rüz, Aurélie Pahud De Mortanges, and Mauricio Reyes. Explainable ai in medicine: challenges of integrating xai into the future clinical routine. *Frontiers in Radiology*, 5:1627169, 2025. 1, 3
- [34] Paul Rutter. The importance of clinical reasoning in differential diagnosis for non-medical prescribers, nurses and pharmacists. *Clinics in Integrated Care*, 31:100271, 2025. 2
- [35] Andrew H Song, Richard J Chen, Tong Ding, Drew FK Williamson, Guillaume Jaume, and Faisal Mahmood. Morphological prototyping for unsupervised slide representation learning in computational pathology. In *Proceedings of the IEEE/CVF Conference on Computer Vision and Pattern Recognition*, pages 11566–11578, 2024. 1, 3
- [36] Yuxuan Sun, Yunlong Zhang, Yixuan Si, Chenglu Zhu, Zhongyi Shui, Kai Zhang, Jingxiong Li, Xinheng Lyu, Tao Lin, and Lin Yang. Pathgen-1.6m: 1.6 million pathology image-text pairs generation through multi-agent collaboration, 2024. 3
- [37] Yuxuan Sun, Yixuan Si, Chenglu Zhu, Kai Zhang, Zhongyi Shui, Bowen Ding, Tao Lin, and Lin Yang. Cpathagent: An agent-based foundation model for interpretable high-resolution pathology image analysis mimicking pathologists’ diagnostic logic. *arXiv preprint arXiv:2505.20510*, 2025. 1, 2, 3

- [38] Xiangru Tang, Anni Zou, Zhuosheng Zhang, Ziming Li, Yilun Zhao, Xingyao Zhang, Arman Cohan, and Mark Gestein. Medagents: Large language models as collaborators for zero-shot medical reasoning, 2024. [6](#), [7](#)
- [39] Yi Tang, Kaini Wang, Yang Chen, and Guangquan Zhou. Endoagent: A memory-guided reflective agent for intelligent endoscopic vision-to-decision reasoning. *arXiv preprint arXiv:2508.07292*, 2025. [3](#)
- [40] Qwen Team et al. Qwen2.5 technical report, 2025. [3](#)
- [41] Eleftherios Tzanis, Lisa C Adams, Tugba Akinci D’Antonoli, Keno K Bressem, Renato Cuocolo, Burak Kocak, Christina Malamateniou, and Michail E Klontzas. Agentic systems in radiology: Principles, opportunities, privacy risks, regulation, and sustainability concerns. *Diagnostic and Interventional Imaging*, 2025. [3](#)
- [42] Sheng Wang, Ruiming Wu, Charles Herndon, Yihang Liu, Shunsuke Koga, Jeanne Shen, and Zhi Huang. Pathology-cot: Learning visual chain-of-thought agent from expert whole slide image diagnosis behavior. *arXiv preprint arXiv:2510.04587*, 2025. [1](#), [2](#), [3](#)
- [43] Xiyue Wang, Junhan Zhao, Eliana Marostica, Wei Yuan, Jietian Jin, et al. A pathology foundation model for cancer diagnosis and prognosis prediction. *Nature*, 634(8035):970–978, 2024. [4](#)
- [44] Jiwen Xin, Adam Mark, Cyrus Afrasiabi, Ginger Tsueng, Moritz Juchler, et al. High-performance web services for querying gene and variant annotation. *Genome biology*, 17(1):91, 2016. [5](#)
- [45] Yingxue Xu and Hao Chen. Multimodal optimal transport-based co-attention transformer with global structure consistency for survival prediction. In *Proceedings of the IEEE/CVF international conference on computer vision*, pages 21241–21251, 2023. [3](#), [6](#)
- [46] Jiawen Yao, Xinliang Zhu, Jitendra Jonnagaddala, Nicholas Hawkins, and Junzhou Huang. Whole slide images based cancer survival prediction using attention guided deep multiple instance learning networks. *Medical Image Analysis*, 65: 101789, 2020. [6](#)
- [47] Wenchuan Zhang, Jingru Guo, Hengzhe Zhang, Penghao Zhang, Jie Chen, Shuwan Zhang, Zhang Zhang, Yuhao Yi, and Hong Bu. Patho-agenticrag: Towards multimodal agentic retrieval-augmented generation for pathology vlms via reinforcement learning, 2025. [1](#), [2](#)
- [48] Yilan Zhang, Yingxue Xu, Jianqi Chen, Fengying Xie, and Hao Chen. Prototypical information bottlenecking and disentangling for multimodal cancer survival prediction. *arXiv preprint arXiv:2401.01646*, 2024. [1](#), [3](#)
- [49] Fengtao Zhou and Hao Chen. Cross-modal translation and alignment for survival analysis. In *Proceedings of the IEEE Int. Conf. Comput. Vis.*, pages 21485–21494, 2023.
- [50] Huajun Zhou, Fengtao Zhou, and Hao Chen. Cohort-individual cooperative learning for multimodal cancer survival analysis. *arXiv preprint arXiv:2404.02394*, 2024. [6](#)
- [51] Junjie Zhou, Jiao Tang, Yingli Zuo, Peng Wan, Daoqiang Zhang, and Wei Shao. Robust multimodal survival prediction with the latent differentiation conditional variational autoencoder. *arXiv preprint arXiv:2503.09496*, 2025. [1](#), [3](#)



# SurvAgent: Hierarchical CoT-Enhanced Case Banking and Dichotomy-Based Multi-Agent System for Multimodal Survival Prediction

## Supplementary Material

**Abstract.** Appendix A presents the performance comparison between SurvAgent and existing open-source pathology-specific multi-agent frameworks on the survival prediction task. Appendix B provides the full WSI Attribute Checklist, including detailed medical definitions for each attribute and their relevance to patient prognosis. Appendix C showcases two complete inference case studies, visualizing SurvAgent’s step-by-step analysis over WSI and genomic data and its final reasoning process. Appendix D details the structure and contents of the CoT Case Bank. Appendix E includes all core prompt designs used in SurvAgent. Appendix F describes the implementation details and experimental settings used to construct and evaluate SurvAgent. The source code will be released for public access.

### A. Comparison with Pathology Multi-Agent Framework

We evaluated SurvAgent against pathology-specific multi-agent frameworks, WSI-Agent [28] and Patho-AgenticRAG [47], across five TCGA cancer cohorts (Table 1). Existing frameworks demonstrate limited performance in survival prediction, with overall C-indexes of 0.524 and 0.509, and particularly low values on challenging cohorts such as GBMLGG (0.39 and 0.527). In contrast, SurvAgent consistently achieves superior prognostic accuracy across all datasets, with an overall C-index of 0.713, improving 19.65% over existing methods and up to 0.833 on GBMLGG, representing a gain of 30.6% over Patho-AgenticRAG (0.527). These results highlight that our multi-agent framework effectively integrates multi-modal pathological information and substantially outperforms specialized pathology agents in survival prediction tasks.

### B. WSI Attribute Checklist Overview

In this section, we provide a detailed illustration of the WSI Attribute Checklist used in SurvAgent. Within our framework, whole slide images (WSIs) serve as one of the primary modalities for downstream survival prediction, and a central challenge lies in identifying which microscopic pathological characteristics most strongly influence patient prognosis. To address this, we construct a curated checklist consisting of 16 prognostic histopathological attributes, complemented by an additional global descriptor summarizing the overall characteristics of the current slide. All



WSI Attribute Checklist

**Tumor grade:** High-grade  
**Depth of Invasion:** Deep muscle invasion  
**Lymphovascular Invasion:** Present  
**Perineural Invasion:** Present  
**Lymph Node Metastasis:** 1-2 nodes  
**Margin Status:** Negative  
**Tumor Morphology:** High-grade urothelial carcinoma.....  
**Carcinoma in Situ:** Absent  
**Variant Histology:** Lymphoepithelioma-like  
**Squamous Differentiation:** Focal  
**Glandular Differentiation:** Extensive  
**Micropapillary Component:** Unknown  
**Plasmacytoid Component:** Unknown  
**Sarcomatoid Differentiation:** Focal  
**Lymphocytic Infiltration:** Mild  
**Necrosis Percentage:** 10-30%  
**Summary:** High-grade malignant neoplasm, perineural invasion, abundant lymphocytic infiltration, necrosis.....

Figure 1. Overview of the WSI Attribute Checklist

attributes are automatically extracted from WSIs by PathAgent and compiled by the Search Agent, which aggregates their definitions and clinical relevance based on pathology guidelines and established medical literature. An example of the full checklist is shown in Fig. 1, and the meaning and definition of each attribute are described below.

**Tumor Grade.** A histological assessment of the tumor’s cellular abnormality and proliferation rate. Reflects the intrinsic biological aggressiveness and growth potential of the tumor. A powerful prognostic indicator; high-grade tumors are consistently associated with significantly higher risks of recurrence and progression to invasive disease, whereas low-grade tumors typically follow a more indolent clinical course.

**Depth of Invasion.** The extent to which the tumor infiltrates the bladder wall, ranging from non-invasive mucosal involvement to deep muscular penetration. Reflects the intrinsic aggressiveness and progression stage of the tumor. One of the strongest predictors of survival; deeper invasion is consistently associated with markedly worse overall survival.

**Lymphovascular Invasion (LVI).** Presence of tumor cells within lymphatic or vascular channels. Indicates early



Table 1. The survival prediction performance (C-index) of the specialized pathological multi-agent framework in five TCGA cancer research groups was compared. “\*” indicates the best results from our reimplementation.

Model	BLCA	BRCA	GBMLGG	LUAD	UCEC	Overall
WSI-Agent* [28]	$0.566 \pm 0.062$	$0.568 \pm 0.068$	$0.390 \pm 0.030$	$0.518 \pm 0.083$	$0.577 \pm 0.055$	$0.524$
Patho-AgentRAG* [47]	$0.478 \pm 0.040$	$0.511 \pm 0.083$	$0.527 \pm 0.063$	$0.523 \pm 0.059$	$0.507 \pm 0.085$	$0.509$
SurvAgent	<b><math>0.683 \pm 0.022</math></b>	<b><math>0.695 \pm 0.013</math></b>	<b><math>0.833 \pm 0.029</math></b>	<b><math>0.676 \pm 0.036</math></b>	<b><math>0.676 \pm 0.052</math></b>	<b><math>0.713</math></b>

metastatic potential. LVI is a well-established independent risk factor for distant metastasis and shortened survival.

**Perineural Invasion (PNI).** Tumor infiltration along or around nerve fibers. Suggests highly invasive tumor behavior. Strongly associated with local recurrence and poor long-term outcomes.

**Lymph Node Metastasis.** Involvement and number of metastatic regional lymph nodes. Forms a crucial component of TNM staging. Increasing nodal burden correlates with stepwise reduction in survival probability.

**Margin Status.** Presence (positive) or absence (negative) of residual tumor at the surgical resection margin. Positive margins imply incomplete tumor removal. Strong predictor of local relapse and reduced survival following surgery.

**Tumor Morphology.** Serves as the foundational visual evidence for tumor grading and subtyping. The morphological assessment is critical; high-grade features, including nuclear pleomorphism and frequent mitotic figures, are directly correlated with aggressive clinical behavior, and the identification of specific variant morphologies (e.g., micropapillary, sarcomatoid) carries significant prognostic and therapeutic implications.

**Carcinoma in Situ (CIS).** A high-grade non-invasive flat lesion with strong malignant potential. Often coexists with aggressive invasive disease. The presence (especially extensive) of CIS predicts increased progression risk.

**Variant Histology.** Non-conventional morphological subtypes such as squamous, glandular, micropapillary, sarcomatoid, plasmacytoid, nested, or lymphoepithelioma-like patterns. These variants frequently exhibit distinct biological behaviors. Many variants, particularly micropapillary, plasmacytoid, and sarcomatoid types, are associated with highly aggressive disease and poor survival.

**Squamous/Glandular Differentiation.** Partial or extensive differentiation toward squamous or glandular phenotypes. Represents divergent tumor evolution. Extensive differentiation is associated with advanced disease and inferior clinical outcomes.

**Micropapillary, Plasmacytoid, and Sarcomatoid Components.** Distinct morphologic components reflecting specific aggressive histologic variants. Indicate profound alterations in tumor microarchitecture. These components are widely recognized as markers of extremely poor prognosis.

**Lymphocytic Infiltration.** Degree of immune cell infiltra-

tion within the tumor microenvironment (TME). Reflects host immune response. Higher infiltration levels often correlate with more favorable outcomes, whereas minimal infiltration suggests an “immune-cold” phenotype.

**Necrosis Percentage.** Proportion of necrotic tumor areas. Indicates rapid tumor cell turnover and insufficient vascular supply. Extensive necrosis is a known indicator of aggressive tumor biology and poor survival.

**Summary.** A concise, free-text summarization that provides a comprehensive characterization of the current WSI intended to mitigate limitations of fixed-value attribute sets. Because the checklist attributes are discretized and selected by prior feature-filtering steps, they may omit subtle, rare, or composite histopathological cues and are susceptible to selection or annotation bias. The Summary Attribute is therefore designed to (1) capture additional prognostic signals not well represented by the predefined categorical fields, (2) record observations where multiple features interact or where uncertainty exists, and (3) serve as a corrective, interpretability-focused descriptor that complements the structured attributes for downstream risk stratification.

## C. Case Study Examples of SurvAgent’s Reasoning Process

To further illustrate the detailed reasoning process of SurvAgent, this section presents several representative case studies. These examples demonstrate how the system analyzes both WSI and genomic data, performs multi-level prognostic reasoning, and integrates morphological cues from WSIs with molecular signatures from gene profiles to generate precise risk predictions. Fig. 4 illustrates the core data involved in WSI analysis, gene analysis, CoT Case Bank construction, and the inference pipeline for the patient with case TCGA-XF-A9SU from the BLCA. Fig. 2 and Fig. 3 focus on the inference stage, presenting SurvAgent’s full WSI reports, gene reports, and the complete CoT-based reasoning process.

## D. Construction of the CoT Case Bank

To enable interpretable reasoning and retrieval-augmented inference within SurvAgent, we construct a unified Chain-of-Thought (CoT) Case Bank. This repository stores structured reasoning trajectories across three complementary

levels: WSI-based analysis, gene-level analysis, and integrated WSI–gene reasoning (Fig. 4). Each case follows a standardized schema that includes the assigned risk level, key evidence, and an explicit uncertainty statement, summarizing both the essential prognostic cues and the inherent ambiguity within the reasoning process. The Gene CoT Case Bank captures reasoning grounded in genomic alterations, abnormal expression patterns, and molecular signatures, while the WSI–Gene CoT Case Bank consolidates these perspectives into a coherent, cross-modal prognostic analysis.

## E. Core Prompt Configuration of SurvAgent

In this section, we present the core prompt design of SurvAgent. Fig. 5–8 illustrate the prompt configurations used in the key stages of SurvAgent. Figure 5 presents the prompt used by PathAgent to extract a structured WSI report based on the predefined WSI Attribute Checklist. Figure 6 shows the prompt used by GeneAgent to perform statistical feature analysis and key gene selection across six categories of functional genes, with tumor suppressor genes illustrated as an example. Figure 7 displays the prompt used by the Inference Agent to predict the exact survival time within the coarse survival interval determined in the first-stage reasoning, leveraging retrieved similar cases and the current patient’s summarized reports. Figure 8 presents the prompt used by the Inference Agent in the first-stage inference, where it integrates retrieved analogous cases, the patient’s WSI and gene reports, and predictions from multiple expert survival models to determine the coarse survival interval.

## F. Implementation Details

### F.1. Experimental Setup and Computing Environment

SurvAgent does not require any additional training, and all results are obtained purely during inference. Experiments are conducted on a computation node equipped with 4× NVIDIA RTX A6000 GPUs (48 GB each) and an Intel(R) Xeon(R) Gold 6430 CPU. For all expert survival prediction models used in our framework, WSI features are extracted using CLAM [27] with the patch level set to 1, and all hyperparameters strictly follow the default settings provided in its open-source implementation. The source code will be released for public access.

### F.2. SurvAgent Architecture

The SurvAgent framework is entirely developed in-house without relying on any existing agent frameworks. SurvAgent consists of four specialized agents: the Search Agent, PathAgent, GenAgent, and Inference Agent. Their implementations are described below.

Search Agent is built upon DeepSeek-V3.2 [9], leveraging its web-access capability in combination with a curated pathology knowledge base to generate an initial WSI Attribute Checklist. The resulting checklist is subsequently reviewed and refined by board-certified pathologists.

PathAgent employs PathGen-LLaVA [36] and Qwen2.5-32B-Instruct [40] as its backbone models. PathGen-LLaVA is responsible for producing expert-level pathological descriptions from WSI image patches, while Qwen2.5-32B-Instruct converts these descriptions into structured pathological attributes, integrates them into a unified report, and performs self-critique on the generated chain-of-thought (CoT) to ensure quality and consistency.

GenAgent is built on Qwen2.5-32B-Instruct, which generates structured gene-level summaries, analyzes statistical properties of functional gene categories, and performs CoT quality verification for gene-related reasoning.

Inference Agent is built on Qwen2.5-32B-Instruct, which is used to perform the final coarse survival interval prediction as well as the precise survival time estimation.

### F.3. Implementation of the Hierarchical WSI CoT-Enhanced Case Bank

In processing whole-slide images (WSIs), we first apply CLAM at patch level 1 with a patch size of  $256 \times 256$  to tile the entire slide, followed by filtering background patches. Patch-level cancer cell detection is then performed using the CHIEF pathology foundation model to identify high-risk regions. Based on the attention scores produced by CHIEF, we apply a DBSCAN clustering procedure to aggregate spatially concentrated high-risk patches, using an epsilon of 4 and a minimum cluster size of 10, thereby determining candidate regions of interest.

WSI examination is conducted in a hierarchical manner across three magnifications:  $2.5\times$  (patch level 3),  $10\times$  (patch level 2), and  $20\times$  (patch level 1). After observing each magnification, PathAgent integrates multi-scale information to form the final WSI-level report used for downstream survival prediction. At  $2.5\times$ , PathAgent directly describes the region. At  $10\times$  and  $20\times$ , subregions are generated by re-tiling the parent region using  $512 \times 512$  windows. Due to the large number of high-resolution patches, we perform CoSMining-based filtering.

For this process, the image-based Self-Path Similarity Matrix is computed via cosine similarity between CHIEF-extracted patch features, while the text-based Self-Path Similarity Matrix is constructed by embedding PathAgent-generated descriptions using the text-embedding-3-large model and computing pairwise cosine similarity. After removing highly redundant patches from both modalities, we take the intersection to obtain the final set of informative subregions.

During the transition from  $10\times$  to  $20\times$ , PathAgent au-

tonomously determines whether further magnification is necessary. This behavior is enabled by prompt-based self-reflection, prompting PathAgent to identify uncertainty or ambiguity in its own outputs and decide whether higher-magnification inspection is required.

In the CoT generation stage, PathAgent aligns the multi-scale WSI report with the patient’s ground-truth risk category and survival time to perform reverse reasoning, yielding fine-grained chain-of-thought trajectories that map pathological findings to survival outcomes. To ensure validity, PathAgent further conducts a verification pass in which the CoT is reevaluated without revealing the ground truth, enabling the agent to detect inconsistencies and revise the CoT accordingly.

#### **F.4. Implementation of the Gene-Stratified CoT-Enhanced Case Bank**

For processing genomic data, we follow prior work to categorize genes into six major functional groups: Tumor Suppressor Genes, Oncogenes, Protein Kinases, Cell Differentiation Markers, Transcription Factors, and Cytokines and Growth Factors. Owing to the large number of genes and genomic fragments, we first conduct statistical quantification to capture the global expression patterns of each gene category.

Specifically, genomic information is divided into DNA-level structural variation data (CNV), RNA-level expression data (RNA-seq), and other special genomic fragments. For RNA-seq expression profiles, the mean and median expression values of each gene are computed to characterize the overall expression distribution of the corresponding gene class. For CNV data, we quantify the mutation rate—defined as the proportion of samples exhibiting mutations such as point mutations, insertions/deletions, or amplifications/deletions—to assess the overall structural variability within each gene category.

After statistical quantification, GenAgent performs a high-level analysis of each gene class to understand its global expression characteristics. GenAgent then generates a preliminary class-level gene expression report and identifies specific genes that require additional inspection. For these selected genes, their raw expression values are retrieved, and GenAgent accesses biological function information via the Gene Knowledge Base constructed using the python library `mygene*`. By integrating the statistical summaries with functional gene annotations, GenAgent performs a systematic, coarse-to-fine analysis of expression behaviors, ultimately producing a detailed report for each gene category.

The reports from all categories are then consolidated into a unified genomic feature report, which serves as input for downstream inference. The process for generating chain-of-thought (CoT) explanations follows the same procedure

described in the previous subsection.

#### **F.5. Implementation of the Dichotomy-Based Multi-Expert Agent Inference Module**

The inference process of SurvAgent is conducted in two stages: (1) estimating a coarse survival interval, and (2) predicting the exact survival time. In the first stage, the reasoning of the Inference Agent is enhanced by both retrieval-augmented generation (RAG) and the outputs of multiple expert survival prediction models. In the second stage, for fine-grained survival time prediction, only RAG-based retrieval information is used to augment the inference process.

After obtaining the patient’s integrated WSI report and genomic report, we perform cosine-similarity-based retrieval over the previously constructed WSI-Gene CoT Case Bank to identify the top three most similar historical cases. Each retrieved case provides its WSI report, gene report, and corresponding chain-of-thought (CoT) annotations.

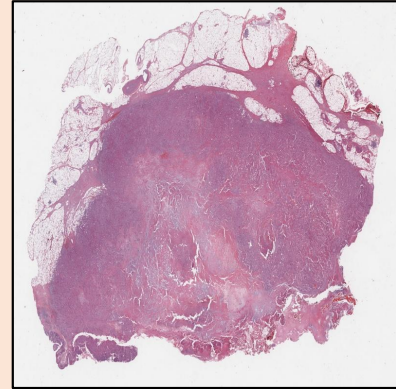
Following the definition of risk scores from expert survival models, we map each model’s predicted risk value into one of four risk strata based on quartiles. These strata align with the target survival intervals: High (0–12 months), High-intermediate (12–24 months), Low-intermediate (24–36 months), and Low (36+ months). The Inference Agent integrates the current patient’s multimodal information, retrieved case evidence, and risk assessments from multiple expert models to determine the patient’s final risk stratum.

Once the coarse survival interval is established, we further retrieve the actual survival times of similar cases. These values are provided as additional prompts to the Inference Agent to facilitate precise survival time prediction at a monthly resolution.

## WSI Summarized Report

Case id: TCGA-XF-A9SJ

"Tumor grade": "High-grade",  
"Depth of Invasion": "There was 4 instance of muscularis propria invasion.",  
"Lymphovascular Invasion": "Absent",  
"Perineural Invasion": "Absent",  
"Lymph Node Metastasis": "not occurred",  
"Margin Status": "Negative",  
"Tumor Morphology": "High-grade urothelial carcinoma with possible sarcomatoid differentiation, adenocarcinoma with glandular differentiation, myxoid stroma, spindle-shaped cells, pleomorphic nuclei, necrosis, invasive fungal infection, heterotopic bone formation, Cryptococcus species, parasitic cystitis",  
"Carcinoma in Situ": "Unknow",  
"Variant Histology": "Sarcomatoid\nGlandular differentiation  
Squamous differentiation\nUrothelial carcinoma",  
"Squamous Differentiation": "Present",  
"Glandular Differentiation": "Present",  
"Micropapillary Component": "Absent",  
"Plasmacytoid Component": "Absent",  
"Sarcomatoid Differentiation": "Present",  
"Lymphocytic Infiltration": "Abundant",  
"Necrosis Percentage": "The necrosis rate in the observed area is 30-50% "



"Summary": "The pathology slide demonstrates a moderately to poorly differentiated adenosquamous carcinoma with glandular structures that moderately deviate from normal architecture, infiltrating the muscularis propria without breaching the serosal surface. The tumor cells exhibit pleomorphism, hyperchromatic nuclei, and cribriform patterns, consistent with adenocarcinoma. Additionally, a densely cellular area with spindle-shaped and epithelioid cells, suggestive of a spindle cell neoplasm such as leiomyosarcoma, is present. The surrounding stroma shows dense collagen deposition, fibroblasts/myofibroblasts, and a desmoplastic reaction. Notable features include areas of necrosis, particularly in the lower right quadrant, and a dense neutrophilic infiltrate indicative of an acute inflammatory response, with abscess formation in the central area. Psammoma bodies are observed, consistent with papillary renal cell carcinoma. The upper left quadrant contains adipocytes and a cluster of cells with a 'pearl necklace' appearance, characteristic of Cryptococcus species, supporting a diagnosis of Cryptococcal infection. Chronic inflammatory processes with lymphocytic and plasma cell infiltrates are also noted. No vascular invasion is observed. Definitive diagnosis requires additional immunohistochemical staining and clinical correlation."

## Gene Summarized Report

Case id: TCGA-XF-A9SJ

The patient's gene cohort demonstrates significant genomic instability with widespread amplifications and deletions across multiple gene groups, including tumor suppressors, oncogenes, protein kinases, cell differentiation markers, transcription factors, and cytokines and growth factors. Notably, tumor suppressor genes such as RB1 and PTEN are downregulated, while CDKN2A shows a low-level gain and upregulation. Oncogenes like FGFR3 and ERBB2 are amplified but downregulated, and MYC is amplified with unknown expression levels. Protein kinases such as MET and AURKA are upregulated, while EGFR and BRAF are downregulated. Key cell differentiation markers like CDH1, GATA3, TP63, KRT20, and FOXA1 are downregulated, indicating an aggressive and undifferentiated tumor state. Transcription factors E2F3 and MYC are amplified, while AR and FOXA1 are downregulated. Cytokines and growth factors such as VEGFA, PDGFRA, IL6, FGF2, EGF, TNF, and IL8 show varying levels of dysregulation, contributing to tumor growth, angiogenesis, and immune evasion. Overall, these findings suggest a complex and aggressive bladder cancer with impaired tumor suppression and dysregulated signaling pathways.

## Final Result

Case id: TCGA-XF-A9SJ

**\*\*Reason\*\*:** The current patient's genomic report indicates significant genomic instability with widespread amplifications and deletions across multiple gene groups, including tumor suppressors and oncogenes. Notably, tumor suppressor genes such as RB1 and PTEN are downregulated, while oncogenes like FGFR3 and ERBB2 are amplified and upregulated. The presence of sarcomatoid and glandular differentiation, along with abundant lymphocytic infiltration and necrosis, further supports an aggressive tumor phenotype. The historical cases (case1, case2, and case3) all exhibit similar aggressive features, including sarcomatoid differentiation, high-grade urothelial carcinoma, and significant genetic instability, with survival times ranging from 2.2 to 4.8 months. Given the high-risk profile and the provided survival time range of 0-12 months, the current patient's prognosis aligns closely with the high-risk category.

**\*\*Risk\*\*:** -0.5786

**\*\*Survival Time\*\*:** 3.54 months

GT: 3.22 months

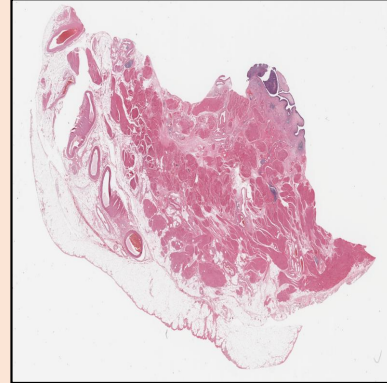
Figure 2. Case studies of SurvAgent, including WSI Summarized report, Gene Summarized report, Final Result, and Survival Time gt (Case ID: TCGA-XF-A9SJ).



## WSI Summarized Report

Case id: TCGA-G2-A2EL

"Tumor Grade": "High-grade",  
"Depth of Invasion": "There was 1 instance of Muscularis propria invasion",  
"Lymphovascular Invasion": "Present",  
"Perineural Invasion": "Absent",  
"Lymph Node Metastasis": "not occurred",  
"Margin Status": "Negative",  
"Tumor Morphology": "High-grade urothelial carcinoma with pleomorphic and hyperchromatic cell clusters, necrosis, hemorrhage, and vascular invasion; papillary and solid growth patterns with dense cellularity and desmoplastic stroma; small cell carcinoma-like areas with small round blue cells, spindle-cell morphology, and high mitotic activity; irregular glandular and cystic architectures formed by atypical epithelial cells with disrupted tissue organization; infiltration of pleomorphic malignant cells with thrombus, necrosis, and hemorrhage; granulomatous and inflammatory responses with lymphoid infiltrates; presence of calcium oxalate crystals; features suggestive of desmoplastic urothelial carcinoma, angiosarcoma, or lymphoma, alongside benign cystic and stratified squamous epithelial components.",  
"Carcinoma in Situ": "Absent",  
"Variant Histology": "Nested\nSarcomatoid\nGlandular differentiation\nSquamous differentiation",  
"Squamous Differentiation": "Extensive",  
"Glandular Differentiation": "Focal",  
"Micropapillary Component": "Absent",  
"Plasmacytoid Component": "Absent",  
"Sarcomatoid Differentiation": "Present",  
"Lymphocytic Infiltration": "Abundant",  
"Necrosis Percentage": "10-30%"



"Summary": "High-grade urothelial carcinoma with necrosis, hemorrhage, and vascular invasion; papillary architecture with hyperchromatic nuclei; small cell carcinoma with hyperchromatic nuclei; spindle cell morphology; small round blue cell tumor; chronic inflammation; lymphocytic infiltrate; dense lymphoid infiltrate, necrosis, calcium oxalate crystals, granulomatous inflammatory response, adenocarcinoma, glandular differentiation, lymphocytic infiltration, disrupted tissue architecture, dense infiltration of atypical cells, pleomorphic nuclei, necrosis, hemorrhage, and thrombus, dense lymphocytic infiltration, reactive or inflammatory process, stratified squamous epithelium, lymphoid neoplasm; necrosis, acute inflammation, fungal hyphae (Aspergillus), parasitic structure, granulomatous reaction, disrupted epithelial layer, inflammatory process with lymphocytic infiltration, necrosis, and foreign body reaction, desmoplastic reaction, possible angiosarcoma, lymphoid aggregates, presence of necrosis, cellular atypia, and dense aggregation of small, round, darkly stained cells; possible carcinoma or lymphoma; high cellularity, hyperchromatic nuclei, and mitotic activity."

## Gene Summarized Report

Case id: TCGA-G2-A2EL

The patient's gene cohort demonstrates significant genetic aberrations indicative of advanced bladder cancer. Notably, there is widespread overexpression of tumor suppressor genes with key genes like RB1, CDKN2A, and PTEN showing downregulation, while TP53 exhibits a low-level gain. Oncogenes show a low-level gain in copy numbers with increased transcriptional activity, though specific oncogenes like FGFR3, EGFR, and ERBB2 are downregulated. Protein kinases exhibit dysregulated states with upregulation of BRAF and MAPK1, but downregulation of EGFR, MET, and AKT1. Cell differentiation markers are generally downregulated, suggesting a poorly differentiated tumor state. Transcription factors show significant dysregulation with E2F3 upregulated and FOXA1, FOXA2, FOXL1, and FOXL2 downregulated. Cytokines and growth factors demonstrate a complex pattern with some genes amplified and others downregulated, indicating reduced signaling activity in the majority of genes. These genetic abnormalities collectively suggest a highly aggressive and complex tumor phenotype.

## Final Result

Case id: TCGA-G2-A2EL

**\*\*Reason\*\*:** The current patient's genomic report and WSI findings indicate a highly aggressive and complex tumor phenotype with significant genetic aberrations, including widespread overexpression of tumor suppressor genes and dysregulated oncogenes. The presence of lymphovascular invasion and abundant lymphocytic infiltration, along with a high-grade urothelial carcinoma with squamous and glandular differentiation, further supports an aggressive tumor behavior. The historical cases provide valuable context: Case 1, despite having a low risk level, shows a more controlled tumor environment with chronic inflammation and fibrosis, which is not the case for the current patient. Case 2, with a high-intermediate risk level, exhibits a similar aggressive phenotype but lacks the lymphovascular invasion noted in the current patient. Case 3, with a high risk level, closely aligns with the current patient's aggressive genetic and morphological features, including carcinoma in situ and squamous metaplasia. Given the authoritative pathologists' provided survival time range of 24-36 months and the historical cases' survival times, the current patient's prognosis is likely to be within the lower end of this range due to the aggressive nature of the tumor.

**\*\*Risk\*\*:** -3.3541  
**\*\*Survival Time\*\*:** 27.34 months

GT: 26.91 months

Figure 3. Case studies of SurvAgent, including WSI Summarized report, Gene Summarized report, Final Result, and Survival Time gt (Case ID: TCGA-G2-A2EL).

WSI CoT Case Bank Case id: <i>TCGA-CF-A3MG</i>	Gene CoT Case Bank Case id: <i>TCGA-CF-A3MG</i>	WSI-Gene CoT Case Bank Case id: <i>TCGA-CF-A3MG</i>
<p><b>Risk Level:</b> High-intermediate</p> <p><b>Key Evidence:</b></p> <ul style="list-style-type: none"> <li>- The presence of high-grade urothelial carcinoma with pleomorphic cells, disorganized architecture, necrosis, and hemorrhage indicates a more aggressive tumor type.</li> <li>- The tumor morphology includes atypical cells forming irregular nests and clusters, pleomorphic nuclei, increased nuclear-to-cytoplasmic ratios, and areas of necrosis and hemorrhage, which are indicative of a higher risk.</li> <li>- The necrosis percentage is between 10-30%, which is significant and suggests a more aggressive tumor behavior.</li> </ul> <p><b>Uncertainty Statement:</b></p> <ul style="list-style-type: none"> <li>- The depth of invasion is non-invasive, which is a positive factor, but the unknown status of lymphovascular invasion, perineural invasion, lymph node metastasis, margin status, tumor number, and tumor size introduces significant uncertainty.</li> <li>- The presence of glandular differentiation and moderate lymphocytic infiltration also adds complexity to the risk assessment.</li> </ul> <p><b>Survival Time:</b> 12.12 months</p>	<p><b>Risk Level:</b> High-intermediate</p> <p><b>Key Evidence:</b></p> <p>The patient's genetic profile demonstrates significant aberrations that contribute to an aggressive bladder cancer phenotype. Notably, the deep deletion and downregulation of CDKN2A, along with the upregulation of RB1, suggest a loss of tumor suppressor function and increased cell proliferation. Additionally, the overexpression or amplification of oncogenes such as FGFR3, MYC, CCND1, ERBB2, and PIK3CA further drive uncontrolled cell proliferation. The downregulation of cell differentiation markers (GATA3, TP63, KRT5, and HOXA13) indicates an undifferentiated and aggressive tumor. These genetic alterations collectively suggest a highly aggressive tumor, but the presence of some downregulated pro-tumorigenic signaling pathways (PDGFRA, IL6, and FGF2) may slightly mitigate the aggressiveness, leading to a high-intermediate risk level.</p> <p><b>Uncertainty Statement:</b></p> <p>None.</p> <p><b>Survival Time:</b> 12.12 months</p>	<p><b>Risk Level:</b> High-intermediate</p> <p><b>Key Evidence:</b></p> <ol style="list-style-type: none"> <li>1. <b>Tumor Morphology</b>: The report indicates a high-grade urothelial carcinoma with pleomorphic cells, disorganized architecture, necrosis, and hemorrhage, which are indicative of an aggressive tumor.</li> <li>2. <b>Genetic Aberrations</b>: The gene report highlights significant genetic alterations, including deep deletion and downregulation of CDKN2A, upregulation of RB1, and downregulation of PTEN. Additionally, overexpression or amplification of oncogenes such as FGFR3, MYC, CCND1, ERBB2, and PIK3CA, along with upregulation of protein kinases like AKT1 and MET, suggest a highly aggressive and undifferentiated tumor phenotype.</li> <li>3. <b>Necrosis Percentage</b>: The presence of necrosis in 10-30% of the tumor indicates a rapidly growing and poorly vascularized tumor, which is often associated with a worse prognosis.</li> </ol> <p><b>Uncertainty Statement:</b></p> <ol style="list-style-type: none"> <li>1. <b>Depth of Invasion</b>: The report states that the tumor is non-invasive, which is a positive factor. However, the status of lymphovascular invasion, perineural invasion, lymph node metastasis, margin status, tumor number, and tumor size are unknown, which could significantly impact the risk level.</li> <li>2. <b>Carcinoma in Situ and Variant Histology</b>: The presence of carcinoma in situ and the specific variant histology are unknown, which could provide additional information on the aggressiveness of the tumor.</li> <li>3. <b>Squamous Differentiation, Glandular Differentiation, Micropapillary Component, Plasmacytoid Component, and Sarcomatoid Differentiation</b>: These factors are also unknown, and their presence could further influence the risk level.</li> </ol> <p><b>Survival Time:</b> 12.12 months</p>

Figure 4. SurvAgent's CoT Case Bank

- You are given multiple **region-level descriptions** from the same Whole Slide Image (WSI) of a bladder cancer patient.

- Given multiple **region-level descriptions** from the same Whole Slide Image (WSI), extract and aggregate **histopathological feature factors** into a single structured JSON output that represents the **overall WSI-level characteristics**, according to the provided **Feature Factor**.

- Please make sure to pay particular attention to the descriptions of certain characteristics that affect the survival time of the patients.

- These structured features will later be used to predict the patient's **overall survival time**, classified into:

- \* A: 0-1 year
- \* B: 1-2 years
- \* C: 2-3 years
- \* D: more than 3 years

- Please only output the final extracted JSON data, without including any other content.

Bladder Cancer Pathology Report:  
{wsi\_report}

List of features to extract: Tumor grade, Depth of Invasion, Lymphovascular Invasion, Perineural Invasion, Lymph Node Metastasis, Margin Status, Tumor Morphology, Carcinoma in Situ, Variant Histology, Squamous Differentiation, Glandular Differentiation, Micropapillary Component, Plasmacytoid Component, Sarcomatoid Differentiation, Lymphocytic Infiltration, Necrosis Percentage, Summary

Please output strictly in the following JSON format, without any additional content:

```
{
  "Tumor grade": "High-grade/Low-Grade",
  "Depth of Invasion": "Non-invasive/Lamina propria invasion/Muscularis propria invasion/Deep muscle invasion/Unknown",
  "Lymphovascular Invasion": "Present/Absent/Unknown",
  "Perineural Invasion": "Present/Absent/Unknown",
  "Lymph Node Metastasis": "None/1-2 nodes/3-10 nodes/>10 nodes/Unknown",
  "Margin Status": "Negative/Positive/Unknown",
  "Tumor Morphology": "...",
  "Carcinoma in Situ": "Present/Absent/Extensive/Unknown",
  "Variant Histology": "Urothelial carcinoma/Squamous differentiation/Glandular differentiation/Micropapillary/Plasmacytoid/Sarcomatoid/Nested/Lymphoepithelioma-like/Unknown",
  "Squamous Differentiation": "Present/Absent/Focal/Extensive/Unknown",
  "Glandular Differentiation": "Present/Absent/Focal/Extensive/Unknown",
  "Micropapillary Component": "Present/Absent/Focal/Extensive/Unknown",
  "Plasmacytoid Component": "Present/Absent/Focal/Extensive/Unknown",
  "Sarcomatoid Differentiation": "Present/Absent/Focal/Extensive/Unknown",
  "Lymphocytic Infiltration": "Minimal/Mild/Moderate/Abundant/Unknown",
  "Necrosis Percentage": "None/<10%/10-30%/30-50%/>50%/Unknown",
  "Summary": "Important descriptions that may affect the duration of survival (Concise medical professional terms)"
}
```

Extraction Rules:

1. Extract strictly based on the report content, do not infer or guess
2. If a feature is not explicitly mentioned in the report, use "Unknown"
3. Ensure all feature values use predefined options
4. Output must be in valid JSON format
5. Pay special attention to bladder cancer-specific pathological features such as carcinoma in situ, variant histology, etc.

Please begin extraction:

Figure 5. The prompt for extracting a structured WSI report using the WSI attribute checklist.

```

## Task
- Below is a description of a patient's basic information, along with statistical sequencing data for the Tumor Suppressor Genes group. Please describe the status of this gene group at the genomic level and indicate whether any abnormalities are present.
- The background knowledge describes the significance of this gene group. You can incorporate this background and your own knowledge of genetics into your analysis.
- In your analysis report, employ medical professional terminology as much as possible for analysis and responses.
- Your output should be as concise as possible! At the same time, it should be comprehensive in analysis, including all the abnormal analyses.

## Background Knowledge
- Significance of the Tumor Suppressor Genes Group: In normal cells, tumor suppressor genes are active and function to inhibit cell proliferation. When these genes are suppressed under certain conditions, or when their sequences are lost, their ability to inhibit proliferation is removed. This allows activated oncogenes to function, leading to abnormal cell proliferation and potentially cancer. In cell cycle regulation, they prevent cells from progressing from one stage to the next, ensuring normal cell division.
- This gene group contains thousands of specific quantified gene sequences. To facilitate your analysis, I will provide their statistical information.
- Genes in this group can be broadly divided into two parts:
1. Gene Copy Number Variation (CNV): CNV refers to a phenomenon where the copy number of a specific DNA sequence in the genome changes relative to the normal reference genome. In normal human cells, most genes are biallelic (2 copies). CNV can lead to an increase (amplification) or decrease (deletion) in the copy number of that segment.
  * Values are typically integers:
  * '-2' = Deep deletion
  * '-1' = Heterozygous deletion (loss of heterozygosity)
  * '0' = Normal copy number
  * '1' = Low-level gain (gain)
  * '2' = High-level amplification (amplification)
2. RNA-seq Characterization: RNA-seq uses high-throughput sequencing technology to measure the transcription level (i.e., mRNA abundance) of each gene within a cell. A high expression level indicates active transcription, while a low level indicates low transcriptional activity.
  * Values are floating-point numbers:
  * Positive numbers = Expression higher than the mean
  * Negative numbers = Expression lower than the mean

## Tumor Suppressor Genes Group Statistics
{Mutation_situation}

{Expression_level_situation}

## Output Example
Abnormal conditions and clinical effects:
1.....
...
n.....
The specific names of the genes that require detailed analysis:
- TP53
- ...
- others genes ... (etc.)

```

Figure 6. The prompt for statistical feature analysis of six categories of functional genes and key gene selection, using tumor suppressor genes as an example.

```

## Task
- Your current task is to predict the future survival time of a bladder cancer patient utilizing the genomic report. You are required to apply your expertise in pathology to accomplish this task.
- You will receive a detailed description of the patient's genomic test results, along with three historical cases retrieved from the case database that most closely align with the current patient's profile. Based on the current patient's report and these historically relevant cases, conduct a thorough analysis to predict the patient's future survival time.
- Meanwhile, for the current case, authoritative pathologists have provided the survival time range for this case. Please use the given information to make the most accurate prediction (to the extent of specific numbers) for the survival time of the current case.
- Your output must consist of an analysis followed by the predicted survival time. Ensure your analysis is concise, clear, and accurate, presented as a coherent paragraph.
- In order to more accurately distinguish the survival time of patients, please retain the predicted survival time to two decimal places.

## Current Patient Report
Genomic Report
{gene_info}
WSI Report
{wsi_info}

## The most likely range of survival time
{time_range} months

## Historically Relevant Cases
"""
case1:
{rag1}

case2:
{rag2}

case3:
{rag3}
"""

## Output Example
Reason: .....
Survival Time: .....

```

Figure 7. The prompt for the Inference Agent to predict exact survival time within the identified interval in coarse survival intervals by retrieved cases and summarized reports.

```

## Task
- Your current task is to predict the future survival time range of a bladder cancer patient using Whole Slide Images (WSI) and genomic reports. You need to apply expertise in pathology to complete this task.
- You will receive detailed descriptions of the patient's whole slide images and genetic test results, along with three historical cases retrieved from the case database that most closely match the current patient's condition. Additionally, you will have access to opinions from four pathology experts who only provide their final conclusions for your reference. Conduct a comprehensive analysis based on the current patient's report and these historically relevant cases to predict the patient's future survival time range.

## Current Patient Report
{patient_info}

**WSI Report**
{wsi_info}

**Genomic Report**
{gene_info}

## Reference Information

### Expert Opinions
Expert 1: {CCL_class}
Expert 2: {MCAT_class}
Expert 3: {MOTCAT_class}

High: Prognostic survival time of 0-12 months
High-intermediate: Prognostic survival time of 12-24 months
Low-intermediate: Prognostic survival time of 24-36 months
Low: Prognostic survival time of over 36 months

### Historically Relevant Cases
====
Case 1:
{rag1}

Case 2:
{rag2}

Case 3:
{rag3}
====

## Please conduct a comprehensive diagnosis based on the following three aspects of information:

### Analysis Phase 1: Independent Feature Analysis
Based solely on the current case features, without considering other information, what is your preliminary judgment and why?

### Analysis Phase 2: Expert Opinion Evaluation
- What is the distribution of expert opinions?
- Are there significant disagreements?

### Analysis Phase 3: Similar Case Reference
- What insights can be gained from the analysis approaches of similar cases?
- What are the key differences between the current case and similar cases?
- How do these differences affect the diagnosis?

### Analysis Phase 4: Conflict Resolution
If there are conflicts among the three information sources:
- Which information source should be prioritized and why?
- How to reconcile contradictions between different information sources?

**Must avoid the following cognitive biases:**
- × Simply following the majority expert opinion
- × Blindly imitating similar case conclusions
- × Relying on external information while ignoring feature analysis

## Output Example
```json
{
  "analysis_breakdown": {
    "feature_based_judgment": "Independent judgment based on features",
    "expert_consensus_analysis": "Expert opinion analysis",
    "case_similarity_insights": "Insights from similar cases",
    "conflict_resolution_strategy": "Conflict resolution strategy"
  },
  "final_prediction": "High/High-intermediate/Low-intermediate/Low",
  "key_decision_factors": [
    "Key decision factor 1",
    "Key decision factor 2",
    "Key decision factor 3"
  ],
  "reasoning_chain": "Complete description of the reasoning chain"
}
...

```

Figure 8. The prompt for the Inference Agent to classify each case into coarse survival intervals by retrieved cases, summarized reports, and predictions from multiple expert survival models.